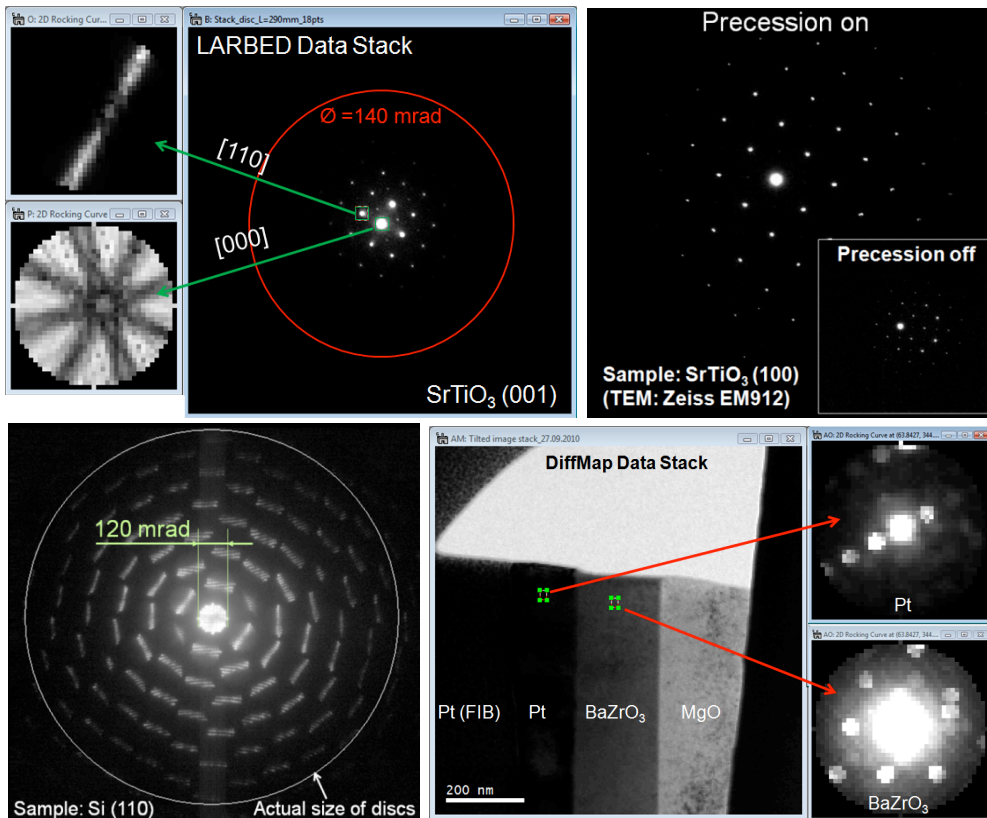


# QED for DigitalMicrograph

Large-Angle Rocking-Beam Electron Diffraction (LARBED)  
Precession Electron Diffraction (PED)  
Diffraction Mapping (DiffMap)  
Fluctuation Electron Microscopy (FEM)



QED Manual 1.2

HREM Research Inc.

## Contact Us

**General enquiries on the QED for DigitalMicrograph should be sent to:**

HREM Research Inc.  
14-48 Matsukazedai  
Higashimatsuyama  
Saitama 355-0055  
Japan

email: support@hremresearch.com  
Website: www. hremresearch.com

**Enquiries on QED of a technical nature should be directed to:**

Prof. Christoph T. Koch  
Institute for Experimental Physics, Ulm University, 89069 Ulm, Germany

email: christoph.koch@uni-ulm.de

## Copyright Statements

© Copyright 2010-2012 HREM Research Inc. and Max Planck Gesellschaft zur Förderung der Wissenschaften

All rights reserved. This manual is protected by international copyright laws and treaties. Unauthorized reproduction and distribution of this manual, or any portion of it, will be prosecuted to the maximum extent possible and may result in severe civil and criminal penalties.

Portions of this document were prepared by HREM Research Inc. by editing the materials supplied by Dr. Christoph T. Koch.

DigitalMicrograph is a trademark of Gatan Inc.

## 1. Introduction:

This QED Manual describes the capabilities and usage of the QED Plug-in for Gatan DigitalMicrograph™ (DM). After giving a short overview of the techniques made available by this plug-in, its usage will be described in detail. A *Quick Reference Guide* explaining the function of each menu and GUI item may be found at the end of this manual.

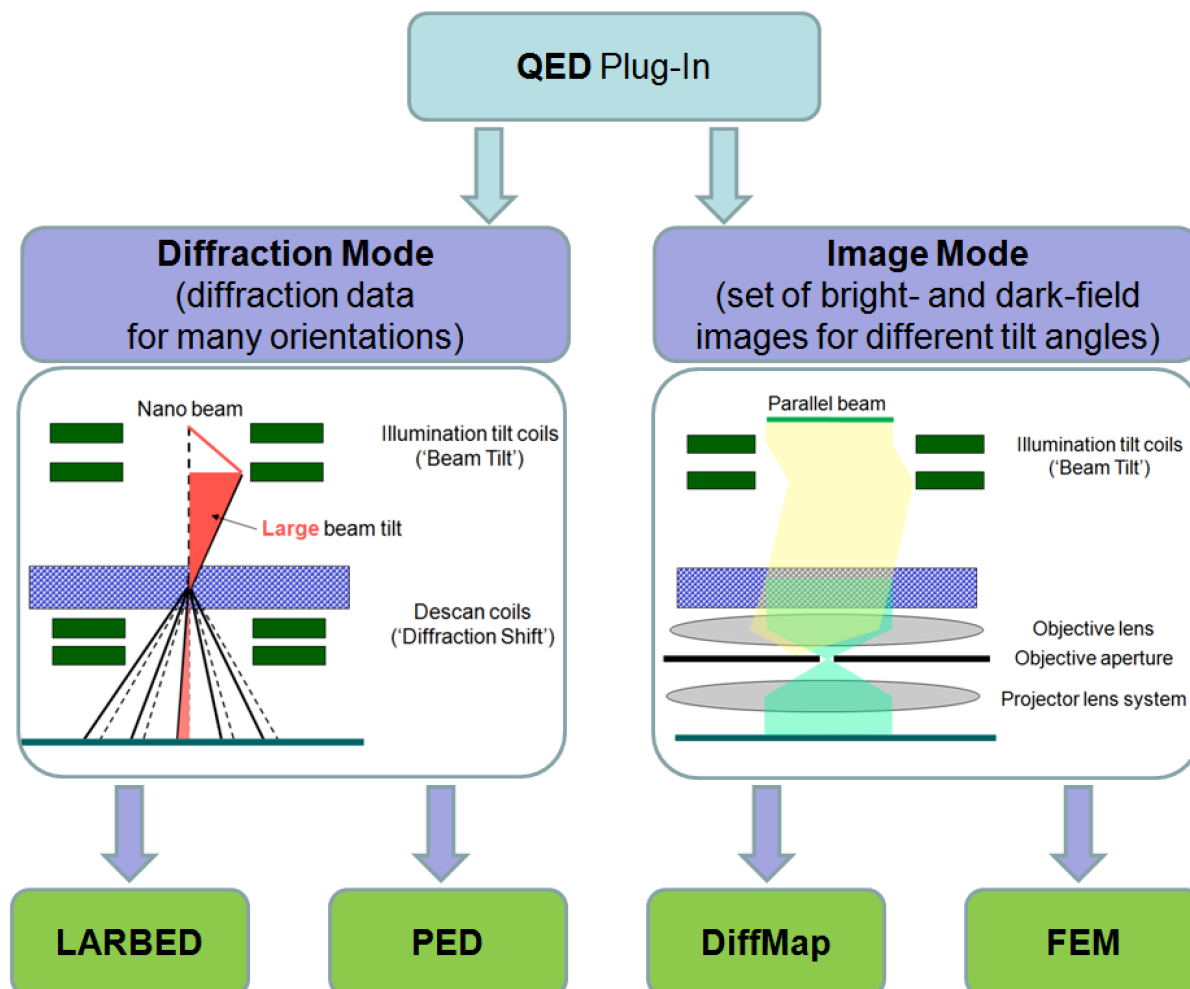


Figure 1: Diagram of TEM/diffraction techniques facilitated by the QED plug-in. While the setup in diffraction mode should be done with a narrow but not highly convergent beam (e.g. in nano-beam diffraction (NBD) mode), in image mode the sample is illuminated by a parallel beam, using the objective aperture to select the reciprocal space resolution.

The QED plug-in provides a number of TEM techniques each of which delivers a specific kind of diffraction information. Figure 1 lists the main acquisition techniques and associated basic data reduction functionality made available by the QED plug-in. More sophisticated data analysis methods are provided by the QEDAnalysis plug-in, which is currently under development.

All of the 4 techniques listed in Figure 1 have been described in the literature. We will therefore not explain them here in detail but only very shortly, pointing to resources for obtaining more detailed information. It is certainly possible to use this plug-in for acquiring the data necessary to obtain information very different from the one targeted by these 4

techniques. The following list therefore only serves to provide a rough idea of what this plug-in can be used for.

**Large-angle rocking-beam electron diffraction (LARBED):** This diffraction technique provides information very similar to convergent beam electron diffraction (CBED) but for ‘semi-convergence angles’ up to (and on some microscopes even in excess of) 100 mrad. This is achieved by recording the different incident beam directions sequentially, instead of in parallel as in the case of CBED using a convergent beam. This technique therefore allows quantitative, background-subtracted CBED-like data to be recorded for crystalline samples that are too thin or have unit cells too large to allow the meaningful application of CBED.

The effect of aberrations and imperfect beam tilt/beam shift separation of the illumination system of the microscope may cause the diffraction spot to illuminate very different regions of the sample for such large beam tilt angles. The QED plug-in therefore implements a sophisticated, fully automated technique for measuring and compensating for these effects, so that all diffraction data indeed stems from the position selected by the user. Further details on the LARBED technique may be found in the references provided below, especially the first one.

1. C. T. Koch, *Aberration-compensated large-angle rocking-beam electron diffraction*, Ultramicroscopy 111 (2011) 828-840
2. C. T. Koch, P. Bellina, P. van Aken, *Software precession electron diffraction*, in: 14th European Microscopy Congress (EMC) in Aachen, Vol. 2: Materials Science, Springer, Berlin Heidelberg, 2008, pp. 201–202.
3. C. T. Koch, *Method and device for measuring electron diffraction of a sample*, United States Patent US 8,076,640 B2.

**Precession electron diffraction (PED):** This technique has been established in 1994 (see the first reference below) and is already associated with quite a large number of published papers. Thus, the references provided below are only a small selection. PED provides electron diffraction data, which can more readily be analyzed using kinematic scattering theory (or rather 2-beam or many-beam theory – see Ref. 8). PED patterns are also relatively insensitive, within a few mrad, to the precise specimen orientation.

The QED plug-in allows the aberration-compensated acquisition of PED patterns by summing up a set of diffraction patterns recorded at a discrete set of beam tilts on a circle. Because of the time for the microscope to respond to remote control commands, this finite sampling is certainly much slower than the continuous sampling provided by a dedicated hardware solution as described in some of the references below (Refs. 1-6). However, the dynamic compensation of aberrations featured by the QED plug-in and the high dynamic range achievable by summing up multiple CCD exposures may compensate this deficit to a large degree.

1. R. Vincent, P. A. Midgley, *Double conical beam-rocking system for measurement of integrated electron diffraction intensities*, Ultramicroscopy 53 (1994) 271–282.

2. M. Gemmi, *Precession technique*, in: J. Puiggali, A. Rodriguez-Galan, L. Franco, M. T. Casas (Eds.), *Electron crystallography and cryo-electron microscopy on inorganic materials and organic and biological molecules*, Barcelona:Universitat Politecnica De Catalunya, 2001, p. L91L97.
3. S. Nicolopoulos, J. P. Morniroli, M. Gemmi, *From powder diffraction to structure resolution of nanocrystals by precession electron diffraction*, *Z. Kristallogr. Suppl.* 26 (2007) 183–188.
4. A. Avilov, K. Kuligin, S. Nicolopoulos, M. Nickolskiy, K. Boulahya, J. Portillo, G. Lepeshov, B. Sobolev, J. P. Collette, N. Martin, A. C. Robins, P. Fischione, *Precession technique and electron diffractometry as new tools for crystal structure analysis and chemical bonding determination*, *Ultramicroscopy* 107 (2007) 431–444.
5. C. S. Own, L. D. Marks, W. Sinkler, *Electron precession: a guide for implementation*, *Rev. Sci. Instr.* 76 (2005) 033703.
6. C. S. Own, *System design and verification of the precession electron diffraction technique*, Ph.D. thesis, Northwestern University (2005).
7. D. Zhang, D. Grüner, P. Oleynikov, W. Wan, S. Hovmöller, X. Zou, *Precession electron diffraction using a digital sampling method*, *Ultramicroscopy* 111 (2010) 47–55.
8. A. S. Eggeman, T. A. White, P. A. Midgley, *Is precession electron diffraction kinematical? Part II: A practical method to determine the optimum precession angle*, *Ultramicroscopy* 110 (2010) 771–777.

**Diffraction Mapping (DiffMap):** A map of diffraction patterns, i.e. a diffraction pattern for a regular array of positions on the sample, may be acquired in two ways (excluding the possibility of numerical nano-beam diffraction from a complex exit face wave function):

- a) sequential sampling of real space by scanning a narrow electron beam across the sample and recording a complete diffraction pattern for each beam position, or
- b) sequential sampling of reciprocal space by using a small objective aperture and recording a series of dark-field (DF) and bright-field (BF) images.

The first option may offer very high reciprocal-space resolution but may result in very long acquisition times, if a large number of real-space points are desired. The second option has generally a rather poor reciprocal-space resolution (determined by the size of the objective aperture) but, because of the parallel acquisition, perfect registration in real space, at least for a single diffraction vector, is achieved. In many cases, also the real-space resolution obtainable by the latter approach is superior to the one obtained by scanning the beam on the sample in the first approach recording individual diffraction patterns. This feature was also taken advantage of in the very interesting application presented in Ref. 5 below.

The QED plug-in facilitates the second approach, including the possibility to define different exposure times for BF and DF images, thus increasing the dynamic range of the reconstructed diffraction patterns and allowing the central beam to be included with the patterns. Because the acquisition of diffraction maps for a large number of reciprocal-space sampling points may take a significant amount of time (20 min up to more than 1 hour), the QED plug-in also provides automated on-the-fly drift compensation. This drift-compensation is achieved by regularly acquiring BF images, measuring the relative drift between successive BF images

and controlling the image-shift coils of the microscope to compensate for the measured specimen drift. Because it is based on the BF images of unchanged contrast this approach is very reliable. Furthermore, compensating any specimen drift via the image-shift coils has the additional advantage that it preserves the full field of view.

1. D. J. Dingley and M. M. Nowell, *The use of electron backscatter diffraction for the investigation of nano crystalline materials and the move towards orientation imaging in the TEM*. *Microchim. Acta* 147 (2004) 157–165.
2. D. Dingley, *Method and apparatus for determining crystallographic characteristics*, US Patent No. 5,576,543
3. D. J. Dingley, *Orientation Imaging Microscopy for the Transmission Electron Microscope*. *Microchim. Acta* 155 (2006) 19–22.
4. G. Wu and S. Zaeferrer, *Advances in TEM orientation microscopy by combination of dark-field conical scanning and improved image matching*. *Ultramicroscopy* 109 (2009) 1317–1325.
5. C. Li and D. B. Williams, *A new TEM method of interfacial thin film characterization*. *Journal of Electron Microscopy* 54 (2005) 57–60.

**Fluctuation Electron Microscopy (FEM):** Just as for diffraction mapping, it is possible to acquire fluctuation electron microscopy data by either sequential sampling of real space and parallel recording of diffraction in reciprocal space (a large number of diffraction patterns) or sequential sampling of reciprocal space and parallel recording of image in real space (a set of hollow-cone DF-images for a set of different illumination tilt angles). Both approaches have traditionally been implemented (see references below).

The QED plug-in allows FEM data to be recorded as a well-calibrated series of hollow-cone DF images (i.e., the real-space approach). However, as for this software's implementation of PED, each hollow-cone DF image is the sum of a finite series of DF images acquired at discrete beam tilts with the same deflection angle but equally spaced azimuth. The drift compensation available for diffraction mapping is also applicable when acquiring FEM data.

1. M. M. J. Treacy and J. M. Gibson, *Variable coherence microscopy: a Rich Source of Structural Information from Disordered Systems* *Acta Cryst.* A52 (1996) 212
2. M. M. J. Treacy, J. M. Gibson, L. Fan, D. J. Paterson and I. McNulty, *Fluctuation microscopy: a probe of medium range order*, *Rep. Prog. Phys.* 68 (2005) 2899–2944
3. M. M. J. Treacy, *Fluctuation microscopy: what it is?*, *Microscopy Today* 13(5) (2005) 20-21
4. S. N. Bogle, L. N. Nittala, R. D. Twesten, P. M. Voyles, J. R. Abelson, *Size analysis of nanoscale order in amorphous materials by variable-resolution fluctuation electron microscopy*, *Ultramicroscopy* 110 (2010) 1273–1278

## **2. Installation:**

The installation of the QED plug-in is achieved by simply copying the files 'QED.gtk', 'QEDlib.gt1' and 'QED.dll' to the 'PlugIns' folder within your DM installation (e.g. 'C://Program Files/Gatan/DigitalMicrograph/' for GMS 1.x). If you install QED for GMS 2.x in a 64-bit system you will need to copy the files 'QED64.gtk', 'QEDlib64.gt1', and 'QED64.dll' to the corresponding folder. On a 32-bit system running GMS 2.x the filenames contain '32' instead of '64'. It is also important that the *IPU plug-in* (compatible with your GMS version) is installed as well. After these files have been copied, DM must be restarted for these changes to take effect. Note that if you have already installed the 'QEDtest.gt2' you may already have the file 'QEDlib.gt1' installed. You may keep the file 'QEDtest.gt2' to test or check your system in future.

Please note that QED.dll will only be loaded by DM, if the USB dongle provided with the QED software is installed at the time DM is started. This DLL is essential for proper functionality of the QED acquisition GUI (see Figure 3). However, off-line data reduction using the QED menu can be done without the USB dongle.

Note: The driver for the USB dongle should be installed following the instructions of the driver installer. However, for off-line data processing it is not necessary to install the file QED.dll as well as the USB dongle driver.

### 3. Getting Started:

Once the plug-ins have been installed, DM's main menu will contain an additional menu item, called 'QED' that has a set of commands shown below.

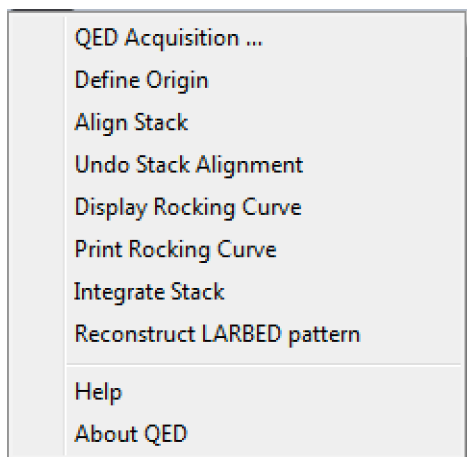


Figure 2: Menu created in DigitalMicrograph by installing the QED.gt1 plug-in. In case the QEDtest.gt2 plug-in is also installed, the menu item "QED test ..." will appear at the top as well.

Selecting 'QED Acquisition ...' will open the following QED acquisition GUI.

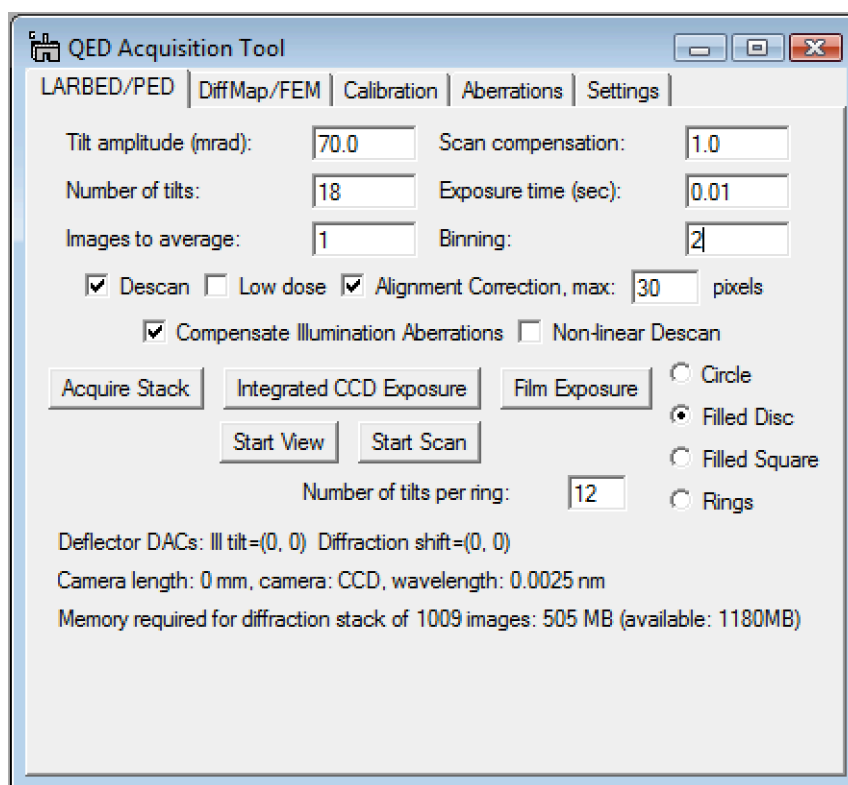


Figure 3: Screen shot of the acquisition tool that opens when starting 'QED Acquisition ...'.

While all functions within the QED acquisition tool are protected by the USB dongle, the other items in the QED menu are also available without the dongle being installed. This allows data that has been recorded on the microscope to be processed using the basic data reduction methods provided by the QED plug-in on a separate computer on which this dongle



has not been installed. For such offline processing it is also not necessary to install the file QED.dll.

Before acquiring your first LARBED, PED, DiffMap, or FEM data set, it is important to run at least the automated beam-tilt calibration routine. For the acquisition of LARBED or PED data sets, it is also recommended to run the aberration calibration routines as well. These acquisition routines will also work without aberration compensation, but there is no guarantee that all the information you obtain will stem from the same area you illuminate with the beam along the microscope's optic axis.

If you perform a LARBED or PED experiment for the first time, you typically need to follow the following procedure:

1. Setup the desired illumination conditions (select spot size and intensity)
2. Calibrate Beam Tilt and descan (in DIFF mode – section 4.1)
3. Calibrate Beam Shift (in IMG mode – section 4.3)
4. Calibrate the illumination aberrations (in IMG-mode, e.g. using the DF-option – section 5.4)
5. Calibrate the Beam Shift-induced Tilt (in DIFF mode – section 4.2)
6. Start your LARBED or PED experiment (chapter 6)

For this reason, after introducing the automated calibration functions for deflectors, the calibration and measurement of pseudo aberration coefficients will be discussed, before explaining the actual acquisition procedure.

## 4. Calibration of the deflection systems:

4.1. Diffraction calibration: When starting the acquisition of LARBED or PED patterns at a camera length for which no calibration has been created yet, a message box (see Figure 4) will appear which reminds the user to first calibrate the beam tilt- and de-scan coils before acquiring diffraction data. Note that these calibrations are also high voltage and camera dependent. On a system featuring more than one CCD camera, QED will require separate calibrations for each detector on which you want to acquire diffraction data. Also when changing the accelerating voltage of the microscope, QED will ask for a separate calibration. All calibration data is stored in DM's global tag structure under 'QED:Calibration:[high voltage]:[camera name]', where the square brackets must be replaced by the actual settings.

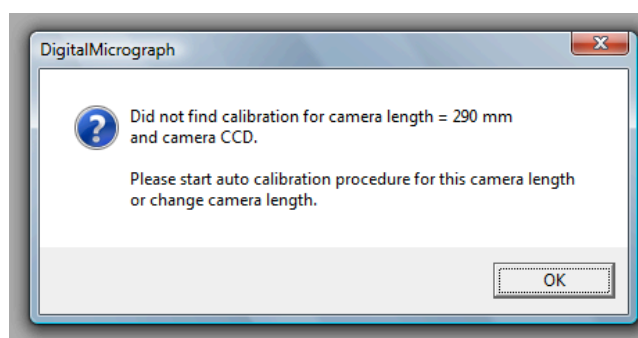


Figure 4: Message box that will appear at an attempt to acquire data if an un-calibrated diffraction setting is encountered.

The diffraction-mode calibration is best done with the sample removed from the field of view. The diffraction pattern will then consist of the undiffracted beam only. Some of the examples shown below have been recorded in this way. The intensity of the diffraction pattern should be adjusted so that it does not severely over-expose the CCD camera. **It is important to select the exposure time and binning such that the CCD will not be damaged!** This may be verified by running the CCD camera in view mode (**make sure to stop the view mode before acquiring your data or starting the calibration!**). The same exposure time and binning should then be used as the **Exposure time** and **Binning** settings in the **Diffraction Calibration** box in the **Calibration** tab (see Figure 5) and the **LARBED/PED** tab (see Figure 23). Note that changing the exposure time for diffraction data in the **Calibration** tab also changes it in the **LARBED/PED** tab and the other way around. The same relation exists between **Exposure time** and **Binning** in the **Imaging Calibration** box and the **DiffMap/FEM** tab. The value set for the number of **Images to average** has no effect for the calibration, where it will always be set to 1.

Users who know what they are doing may also specify **Tilt amplitude** in DAC (digital-to-analog control) units for the calibration. However, it is suggested to simply leave this value at '0', because in that case the calibration routine will automatically determine a value that corresponds to 1/2 of the available field of view in either direction for any camera length.

The **Correlation threshold** indicates the smallest acceptable value of the maximum found by the feature-tracking algorithm. If no peak above this threshold can be found then the calibration will be aborted. Such failure of the calibration routine can occur, if an objective

aperture is obstructing the direct beam of the diffraction pattern, or the diffraction pattern has shifted out of the field of view, e.g. by specifying too large a value for **Tilt amplitude (DACs)**.

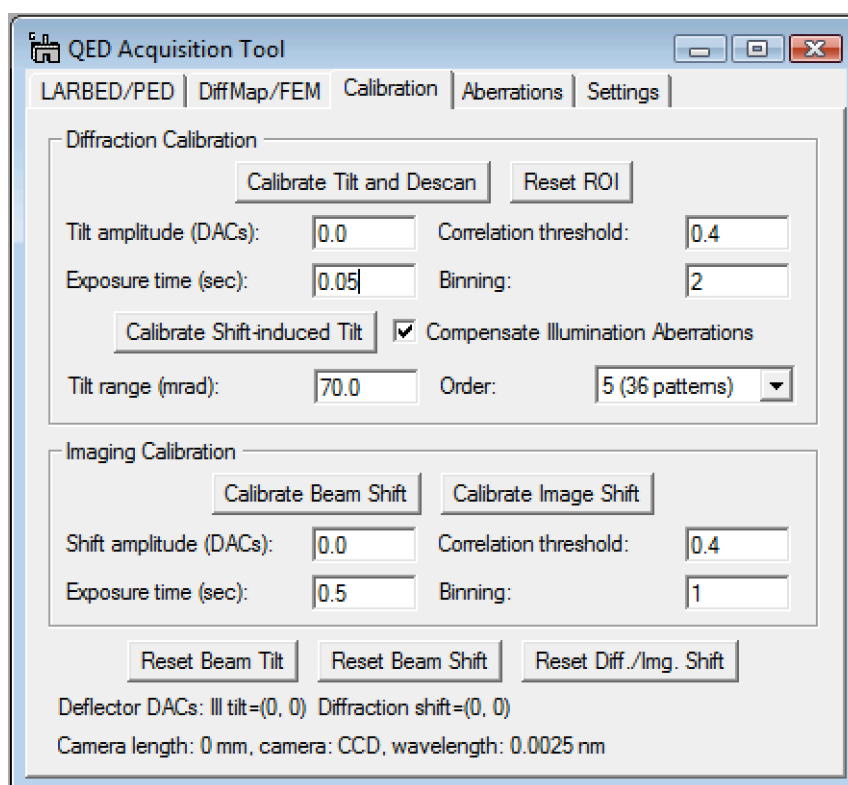


Figure 5: The **Calibration tab** of the QED Tool. This shows the experimental conditions and buttons relevant for calibrating the beam tilt, tilt de-scan, and beam-shift-induced beam tilt as well as the beam shift and image shift. It also provides a few buttons to reset the illumination tilt and diffraction shift for the unlikely case that this is needed.

The QED calibration relies on DM's calibration of diffraction patterns, i.e. it requires that diffraction patterns are calibrated in the units ' $1/\mu\text{m}$ ', ' $1/\text{nm}$ ', or ' $1/\text{\AA}$ ' using a known sample. Only then can the software properly calibrate and apply the illumination tilt .

Pressing the **Calibrate Tilt and Descan** button will launch the fully automated calibration procedure for the beam tilt and the tilt de-scan. This procedure will first produce a continually updating image of the diffraction pattern. The user is then asked to move the central spot of the diffraction pattern well inside the region of interest (ROI) defined in the image. Alternatively, one may also move the ROI to the central spot and/or re-size the ROI. However, one should not move the ROI too far from the image center, because otherwise the calibration routine may shift the diffraction pattern outside the area captured by the CCD. Pressing the **Reset ROI** button will reset the size of the selection to 1/8 of the field of view of the whole detector and position it at the center of the view window. It is then a very simple task to move the diffraction pattern to the center of the detector.

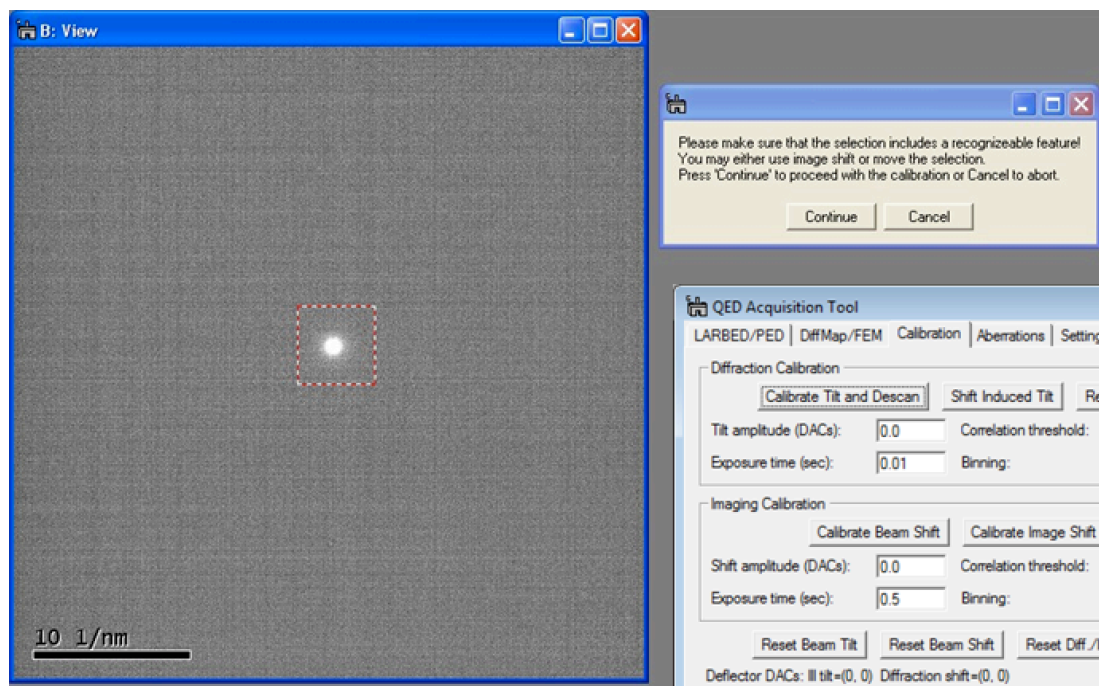


Figure 6: Screen shot demonstrating how the diffraction pattern should be set up for running the automated calibration routine.

Once the user has brought the central beam within the ROI, the actual calibration may be started by pressing the ‘Continue’ button which should finish with the message ‘Calibration successful’, as shown in Figure 7.

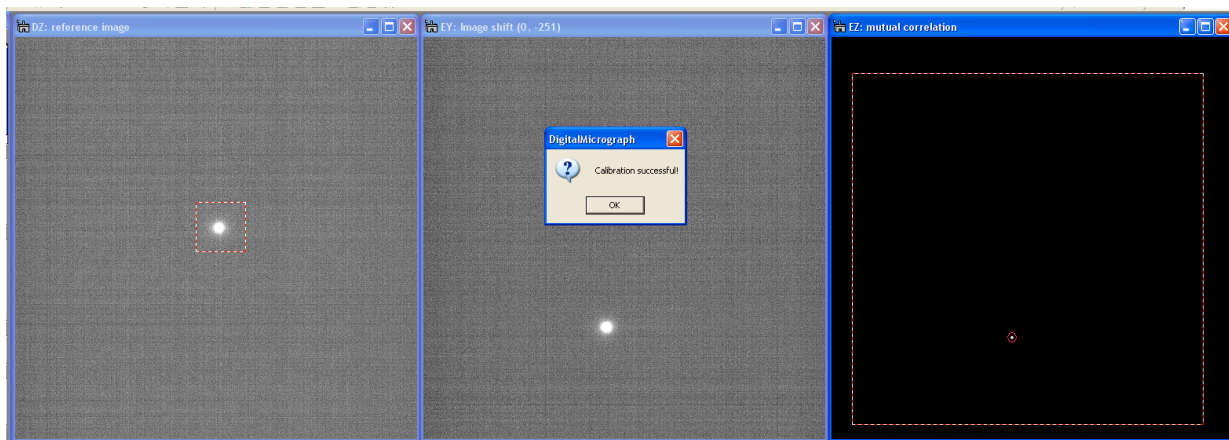


Figure 7: Screen shot of the 3 images shown at the point of completion. The image on the left is the reference image, the image in the center shows the tilted or shifted diffraction pattern, and the one on the far right shows a special correlation function used to measure the relative shift between the two images. Acknowledging the completion of the calibration by pressing ‘OK’ will automatically close all of these three windows.

**4.2. Calibration of shift-induced tilt (non-linear de-scan):** The diffraction shift calibration procedure described in section 4.1 only measures the diffraction shift along two orthogonal directions. If both the beam tilt and the diffraction shift behave in a fully linear manner, this calibration would be sufficient. However, it turns out that, although much smaller deviations from the optic axis are involved, on most microscopes the diffraction shift does not behave in a fully linear fashion. As shown in the example in Figure 8 (recorded on the Zeiss SESAM for a tilt amplitude of 60 mrad ( $\approx 3.4^\circ$ )), assuming the applicability of a simple linear

calibration may result in delocalized scan figures in PED patterns at large precession angles or in distorted discs in LARBED patterns for large LARBED disc radii, as shown in the left hand column of Figure 8. This problem can be overcome by applying a non-linear calibration scheme which is, similar to the illumination aberration compensation described in chapter 5, based on a larger number of diffraction tilts, spiraling all the way up to tilt amplitudes used for acquiring the actual experimental data. Applying such non-linear calibration scheme compensates any residual movement (beyond the precision limitations imposed by the remote control interface used by DigitalMicrograph to control the microscope deflection coils) of the diffraction pattern with beam tilt, as demonstrated in the right hand column of Figure 8.

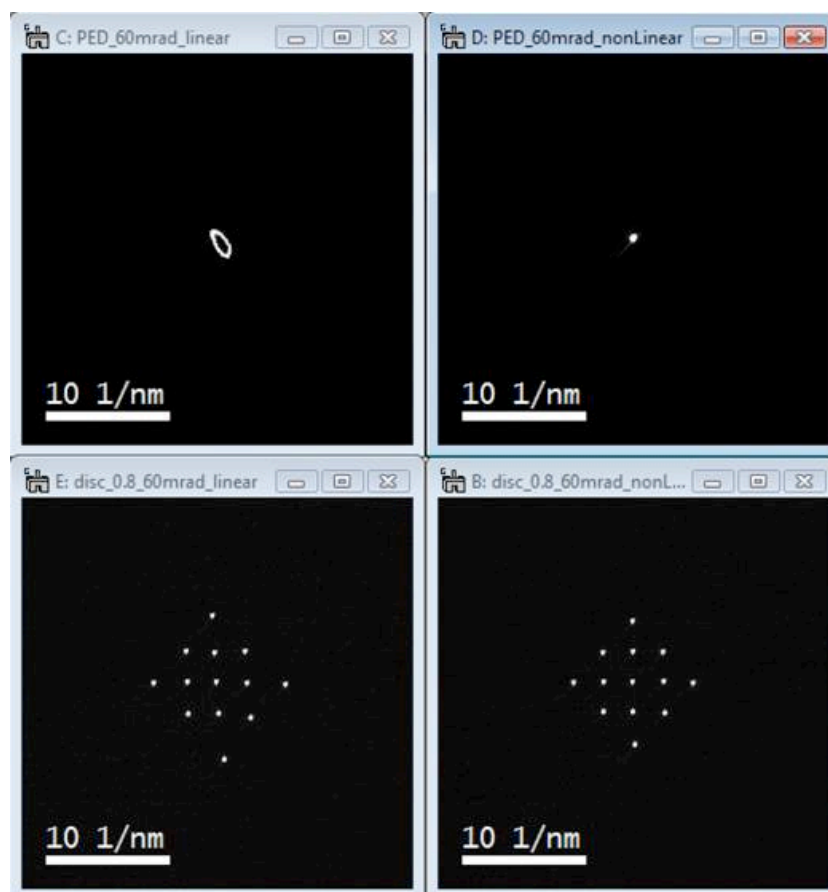


Figure 8: Comparison of PED (top row) and LARBED patterns (bottom row) acquired using a linear (left column) and non-linear (right column) diffraction shift calibration on the Zeiss SESAM. The tilt range was set to 60 mrad in all four patterns.

This non-linear de-scan calibration may be performed right after the **Tilt and Descan** calibration. However, it also serves another purpose: On many microscopes the compensation of aberration-induced probe wandering described in chapter 5 also introduces additional beam tilt which may then also distort the scan pattern recorded on the CCD camera. If the **Shift-induced tilt** calibration is performed after the calibration of the illumination pseudo-aberrations it will also compensate shifts in the diffraction pattern caused by this additional beam tilt. If the **Compensate Illumination Aberrations** option is turned off, then the beam will not be shifted during this calibration. It is strongly recommended to perform this calibration with the same setting of the **Compensate Illumination Aberrations** option as used when acquiring the actual experimental data.

The experimental setup for calibrating the Shift-induced tilt is identical to the one described in section 4.1. The user then has the choice to either apply this non-linear calibration during data acquisition, or not.

**4.3. Beam shift calibration (Imaging calibration):** In order to shift the beam for compensating aberrations of the illumination system, one must first calibrate the amount of shift induced by the beam shift coils. This calibration is done automatically when the **Calibrate Beam Shift** button in the **Calibration tab** is pressed.

The beam shift calibration requires a small field of illumination, say not much more than 1/8, compared to the size of the whole CCD detector (not much bigger than shown in Figure 9). As for the calibration of the beam tilt and tilt de-scan, the spot should also be positioned close to the center of the CCD using either the beam shift or the image shift coils or by moving the condenser aperture. Electron optically, it is in most cases best to keep the electron beam as close as possible to the optic axis. The last option may therefore be the preferred one, assuming that the beam shift and image shift are already at their optimized settings.

Even if the image of the condenser aperture is not completely centered or even the condenser aperture is not inserted, pressing the **Calibrate Beam Shift** button in the **Calibration tab** will provide opportunity to center the illumination spot. Pressing **Continue** in the dialog box that will appear (similar to Figure 6 for the case of the diffraction calibration) will proceed with the calibration, but pressing **Cancel** will abort it. Note that typically a longer exposure time may be selected for calibrations based on the acquisition of images than for diffraction patterns.

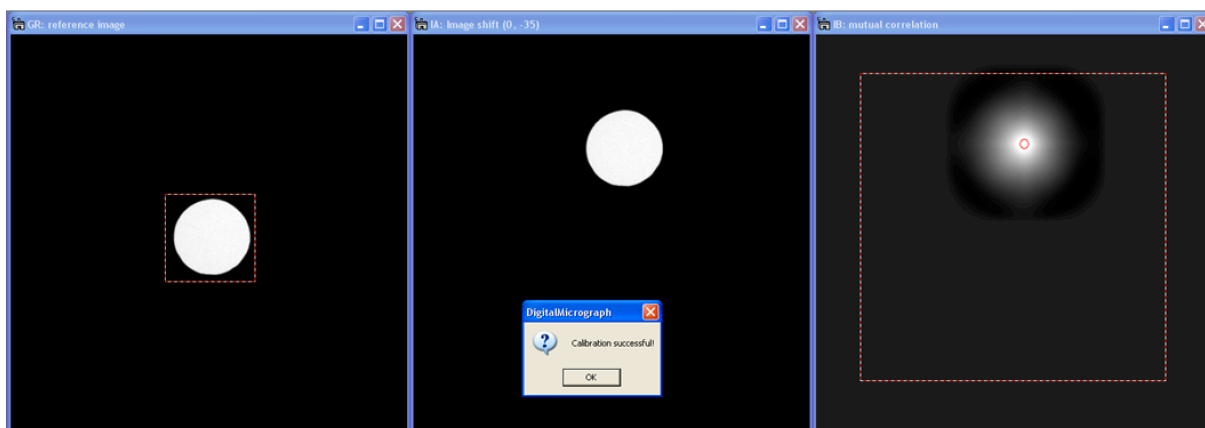


Figure 9: Screen shot of the beam shift calibration wizard at the point of completion. The large square superimposed on the correlation window shows the valid range within which feature defined by the small selection in the reference image may be located. The little red circle indicates the position of the highest correlation found within this range of validity. Acknowledging the completion of the calibration by pressing 'OK' will automatically close all of these three windows.

**4.4. Image shift calibration (Imaging calibration):** The calibration of the image shift works in the same way as the beam shift calibration. It may be run again with a small condenser aperture, or, alternatively, without condenser aperture but a sample with an easily trackable feature positioned at the center of the CCD. The simplest way is probably to just press

**Calibrate Image Shift** after completion of the beam shift calibration without changing anything regarding the alignment of the microscope or the sample position.

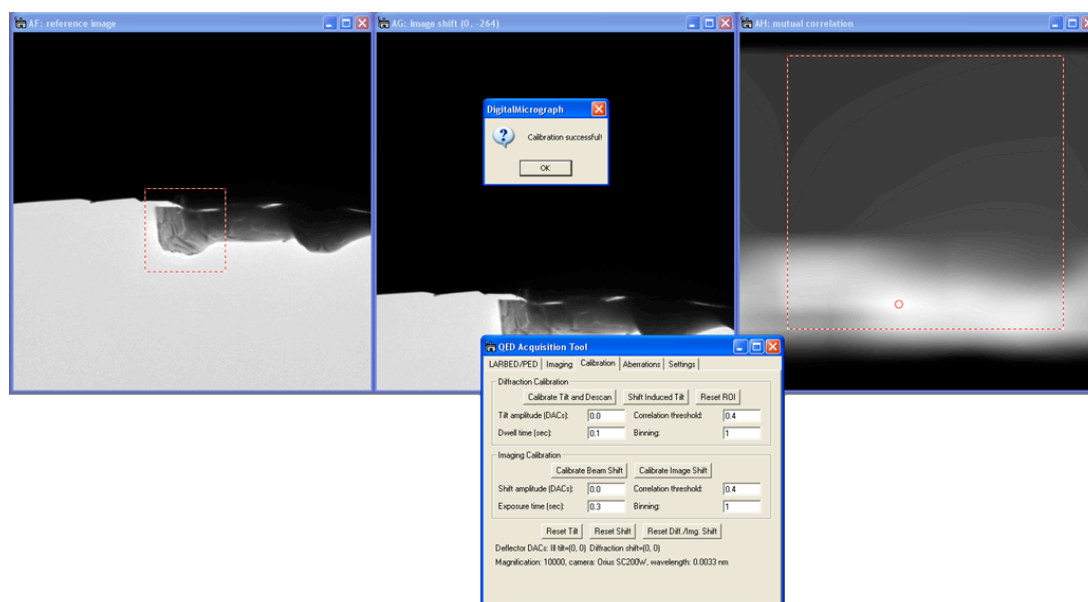


Figure 10:: Screen shot of the image shift calibration procedure showing the reference image, the current (shifted) image, and the correlation of the two. The large square super-imposed on the correlation window shows the valid range within which feature defined by the small selection in the reference image may be located. The little red circle indicates the position of the highest correlation found within this range of validity. Acknowledging the completion of the calibration by pressing ‘OK’ will automatically close all of these three windows.

Note that the image shift calibration is important for measuring the pseudo-aberration coefficients of the microscope in BF mode, but not in DF mode. If the image shift has been calibrated for the current magnification, the aberration measurement will be much more robust because image drift out of the field of view of the detector will be avoided then. For calibrating pseudo-aberrations of the imaging system in BF-mode *a magnification range between 10 kx and 30 kx is recommended.*

Furthermore, the image shift calibration is essential for a prolonged image-mode data acquisition for DiffMap or FEM, where automated on-the-fly drift compensation will be crucial. For acquiring DiffMap or FEM data the image shift must be calibrated *at the same magnification* as used for the data acquisition.

## **5. Correcting Aberrations of the illumination system:**

### 5.1. Background:

Transmission electron microscopes *equipped with an aberration corrector* for the illumination system are ideal for precession electron diffraction, because they allow the electron beam to remain in the same position even at quite large (currently up to about 50 mrad) precession angles<sup>1</sup>.

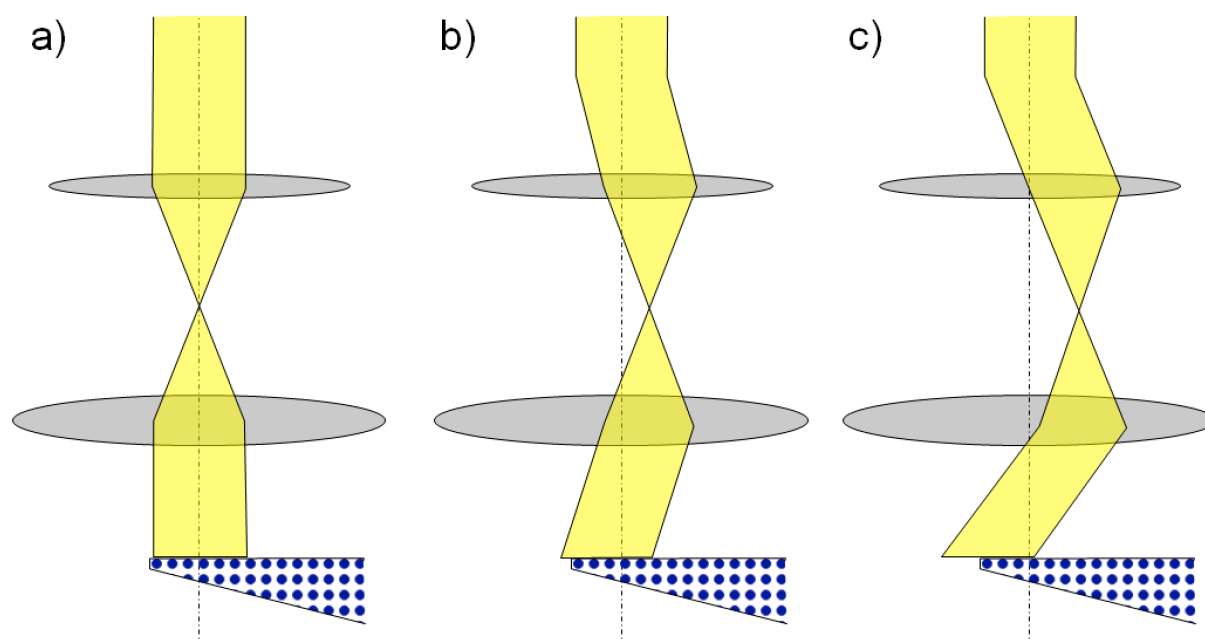


Figure 11: Schematic of the optical path in the illumination system of the TEM: a) untilted illumination b) tilted illumination with  $C_s > 0$  for a small tilt angle.. c) tilted illumination with  $C_s > 0$  for a large tilt angle. The spherical aberration causes the field of (parallel) illumination to shift proportional to the third power of the deflection angle.

However, this is not the case for a regular TEM without an aberration corrector as illustrated in Figure 11. A positive spherical aberration coefficient of the objective pre-field lens (or the illumination system in general) causes the beam to shift along the direction in which it has been tilted. Diffraction patterns at different tilt angles may therefore originate from very different areas on the sample. Figure 12 gives a more quantitative idea of how far the illuminating beam will move with illumination tilt angle, given specific values for the aberrations.

<sup>1</sup> C. S. Own, W. Sinkler, L. D. Marks, *Prospects for aberration corrected electron precession*, Ultramicroscopy **107** (2007) 534542



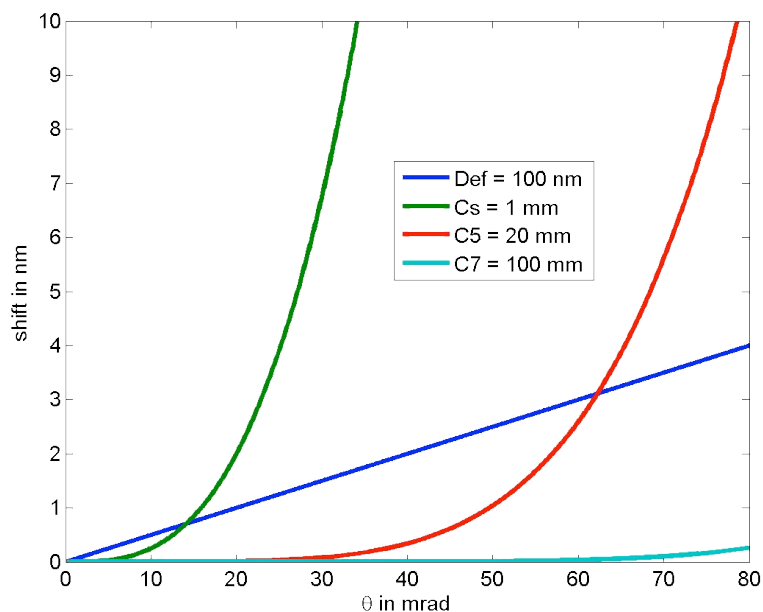


Figure 12: Beam shift induced by various aberrations ( $E_0 = 200$  kV). While the effect of spherical aberration ( $C_s = 1$  mm) is already quite severe at tilt angles  $> 20$  mrad, the 5<sup>th</sup> order spherical aberration ( $C_5 = 20$  mm) only really matters at tilt angles above 50 mrad. Note that on many TEMs not designed for high resolution work, the aberration coefficients may be much larger than those used in this example.

Since the purpose of the LARBED and PED methods is to obtain diffraction patterns from a very well-defined area on the specimen, it is important to compensate the tilt-induced shift of the illuminated area. This compensation may be done by moving back the beam by using the beam shift. It will be described below how the QED plug-in measures all 42 complex-valued pseudo aberration coefficients of the illumination system in a fully-automated fashion. These coefficients are then used to compensate for tilt-induced beam shift during acquisition. Mathematical details regarding the precise formulation of the pseudo-aberration coefficients and their measurement are described in the literature<sup>2</sup>. Here, we will only give a very short explanation. We call these coefficients the imaging and illumination *pseudo*-aberration coefficients, because they mainly correspond to the aberration coefficients of the objective lens (imaging system) and objective pre-field lens (illumination system), respectively. However, they also include the effect of projector lens distortions and imperfections or nonlinearities in the separation of beam tilt and beam shift. Their magnitude also scales with DM's calibration of the acquired images and diffraction patterns. However, even if DM's scale bars are not correctly calibrated at all, as long as they do not change, the pseudo-aberration coefficients obtained by the QED plug-in remain self-consistent and will keep the probe from wandering about your sample – and this is all that they are meant to be used for.

<sup>2</sup> C. T. Koch, Aberration-compensated large-angle rocking-beam electron diffraction, *Ultramicroscopy* **111** (2011) 828-840.

Figure 13 provides an example of a probe shift map produced from a set of illumination pseudo-aberration coefficients measured for the Zeiss SESAM, displayed once as amplitude and angle (top row) and, alternatively, as shift along the two orthogonal directions (bottom row). Applying the probe shift associated with a specific beam tilt (horizontal and vertical axes of the map) will keep the probe always at the same specimen position.

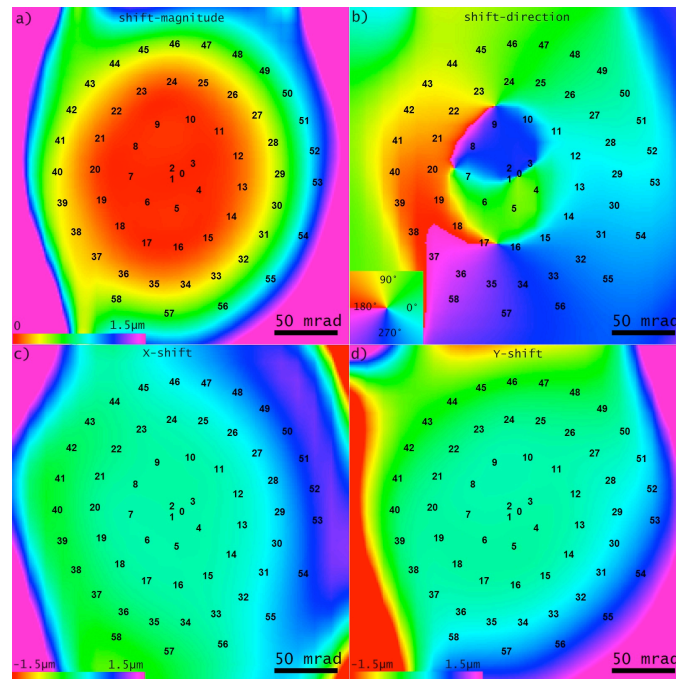


Figure 13: Map of the tilt-induced probe shift on the sample as produced by the QED software, once shown as shift magnitude (a) and direction (b) and, alternatively, as beam shift parallel to the horizontal (c) and vertical (d) axes of the CCD detector. The color scale has been limited to shifts  $\leq 1.5 \mu\text{m}$ . The axes of these maps represent the illumination tilt angle (in mrad, as indicated by the scale bar). The spiral pattern of numbers in each figure indicates the tilt angles of the 59 dark-field images recorded during the automated aberration calibration procedure to determine all 42 complex-valued pseudo aberration coefficients up to 7<sup>th</sup> order. The first 3 images (numbers 0, 1, and 2) were recorded for equal tilt amplitudes of 5 mrad, differing in their azimuth by 120°.

## 5.2. Calibration of pseudo-aberrations in **BF-** or **DF-mode**:

The aberration calibration may be done in two ways: a) first calibrating the aberrations of the imaging system and then calibrating the illumination system and b) calibrating the movement of a small illuminated area on the sample by tracking the position of the on-axis dark-field image on the detector. The latter approach requires an amorphous sample with trackable features in order to have a detectable signal at all tilt angles.

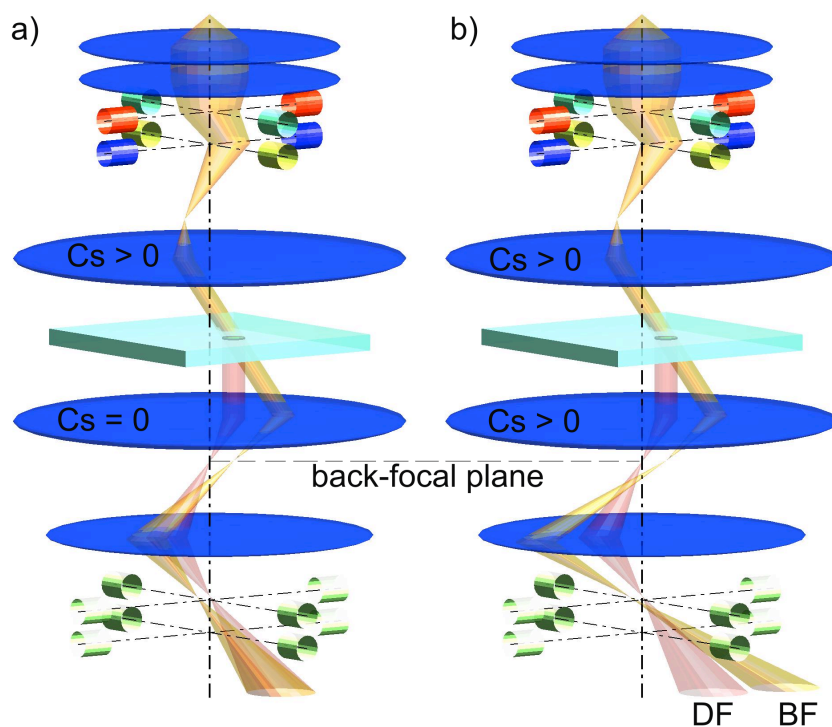


Figure 14: Illustration of the effect of spherical aberration of the objective lens on the measurement of the spot on the sample in the image mode, assuming, for the purpose of illustration, that  $C_s$  is the only significant aberration. a) If  $C_s = 0$  for the imaging system, both the images of the tilted undiffracted beam (yellow beam) and the diffracted beam (red beam) end up at the same position on the detector. b) In an uncorrected microscope (or if the sample is not perfectly focused) images of the diffracted and undiffracted beams are detected as BF and DF images at different positions on the detector.

As illustrated in Figure 14b, aberrations of the objective lens will induce a tilt-dependent image shift of the illuminating probe, exaggerating its actual movement on the sample. As discussed in detail in<sup>2</sup>, when tracking the movement of the illuminating spot on the detector by recording its bright-field (BF) image, it is necessary to characterize the aberrations of the objective lens, in addition to those of the objective pre-field lens. However, if one brings some amorphous sample area within the field of view, inserts a small objective aperture and aligns it with the microscope's optic axis, the movement of the probe on the sample may be tracked directly by following the movement of the dark-field (DF) image of the probe on the sample, independent of the aberrations of the objective lens. Here, the DF image is created by diffracted electrons that pass through the small objective aperture. Either method has some advantages as well as disadvantages, which is why QED offers a choice of either method (BF or DF). While the BF calibration requires both imaging and illumination aberrations to be calibrated, its advantage is that, once the aberrations of the objective lens (the imaging system) have been determined, the aberration calibration of the illumination system may be performed without any sample. The DF method, on the other hand, may be simpler in that it requires only a single calibration step, but it may involve very long exposure times if the scattering of the amorphous sample is weak, which is why QED offers an auto-illumination option for the illumination aberration calibration in DF mode.

### 5.3. Measuring microscope pseudo-aberration coefficients in **BF-mode**:

The calibration of the microscope's aberrations requires that all the relevant calibrations (beam tilt, beam shift and image shift) have been performed beforehand. The aberration calibration in BF-mode is done in at least 2 steps: First the imaging aberrations are calibrated, and then the illumination aberrations can be quantified. This is because the tilt-induced beam shift is amplified by the aberrations of the objective lens, as illustrated in Figure 14 and Figure 15. If the pivot-point of the illumination system is not properly adjusted, or it behaves in a non-linear fashion (to be expected even on a perfectly aligned TEM if the tilt range is sufficiently large, i.e. greater than 50 mrad), applying some beam shift will also induce some beam tilt. The user therefore has the option to refine the pseudo-aberration calibration by repeating these 2 steps again (more on the aberration calibration refinement in section 5.3.3).

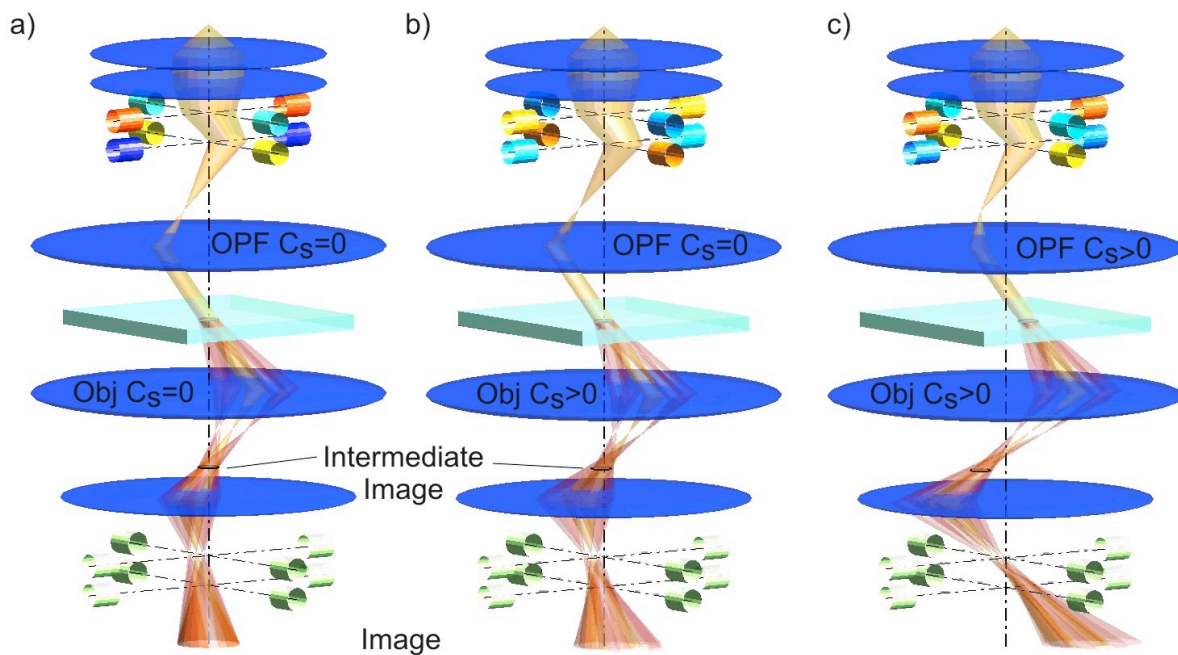


Figure 15: Diagram illustrating the effect of aberrations of both the objective pre-field (OPF) lens as well as the objective lens. a) If the spherical aberration of both lenses is zero, the image as well as the spot on the sample remains well-focused and not displaced, even if the beam is tilted with respect to the optic axis. b) Aberrations of the objective lens have the effect that the intermediate image will shift with beam tilt and also the image on the detector will be shifted and blurred, because the partial image produced by each of the diffracted beams is shifted by a different amount. c) Aberrations of the illumination system will shift the probe on the sample with beam tilt. This shift is amplified by the aberrations of the objective lens so that the apparent movement of the illumination probe in the detector plane is greater than the actual movement of the probe on the sample.

#### 5.3.1 Calibrating aberrations of the imaging system in **BF-mode**

Before starting the measurement of the pseudo-aberration coefficients of the imaging lens system, one should decide on the desired order of aberration compensation. Using a higher aberration order provides higher accuracy because of the larger number of coefficients being fitted but requires more images to be acquired (see Table 1) and thus prolongs the calibration time. Depending on the microscope and size of detector *it is recommended to perform the aberration calibration at a moderate magnification, i.e. below about 80 kx, in some cases as low as 10 kx.*

Also, for calibrating the image aberrations, the objective lens current should be at its nominal value and the sample should be at the eucentric height. It is important to select such reproducible conditions, since the fitted pseudo-aberration coefficients for the imaging system depend on the alignment of the microscope as well as the position of the sample (especially the defocus). The coefficients fitted at the area of the sample will only be valid at the same area in the field of view, if the microscope alignment has not changed in between and the sample is at the same height. Depending on the stability of the microscope and the desired accuracy, however the aberration calibration may then only have to be done once for all future QED sessions.

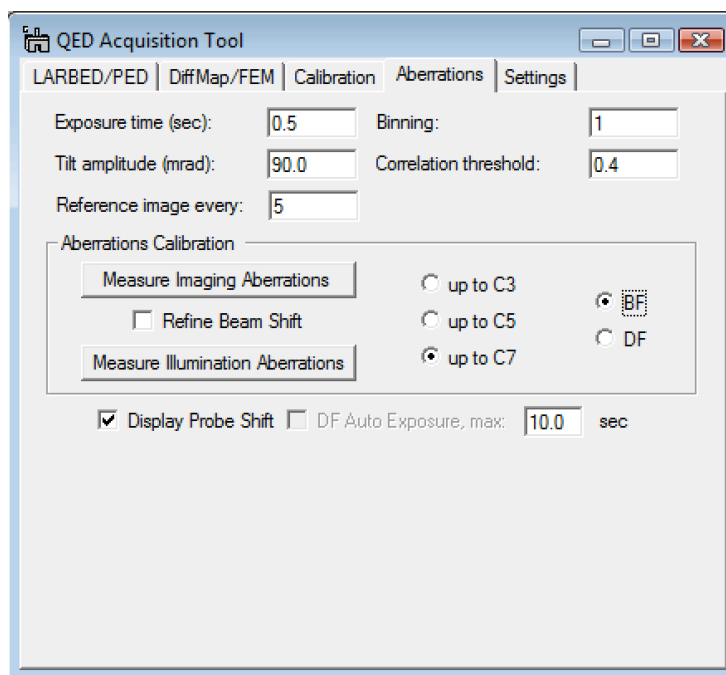


Figure 16: Screen shot of the **Aberrations** tab. Here the BF mode has been selected and specimen drift will be compensated by acquiring on-axis BF reference images after every 5 images at tilted illumination.

Similar to the acquisition of diffraction maps, any specimen drift may be compensated for by acquiring a new BF reference image every few frames. The number of tilted images to be acquired between successive BF reference images may be specified in the field ‘**Reference image every**’ in the **Aberration** tab (e.g. 5 in the example shown in Figure 16). Choosing a small number results in a more robust measurement in the presence of specimen drift but will also slightly prolong the total acquisition time for this calibration procedure.

Pressing the **Measure Imaging Aberrations** button in the **Aberration** tab will start the corresponding automated calibration routine. As for the case of the other calibrations, the software will first pop-up the dialog as shown in Figure 17 asking the selection to be repositioned and adjusted in size to define a trackable area of the sample. Once the **Continue** button has been pressed a series of tilted images will be acquired. The number of images depends on the selected order of pseudo-aberration coefficients to be fitted (i.e. up to C3, C5, or C7) and is given in Table 1. *If the illumination aberrations have not been calibrated yet, the **Refine Beam Shift** checkbox should **not** be selected.*

Aberration order	Number of pseudo-aberration coefficients	Number of images required
up to C3	12	20
up to C5	25	36
up to C7	42	57

Table 1: List of the number of pseudo-aberration coefficients being fitted to the tilt-induced image- or beam-shift and the number of images acquired by the calibration routines to determine these coefficients. Note that each of the pseudo-aberration coefficients is complex-valued, i.e. it has an amplitude and a phase.

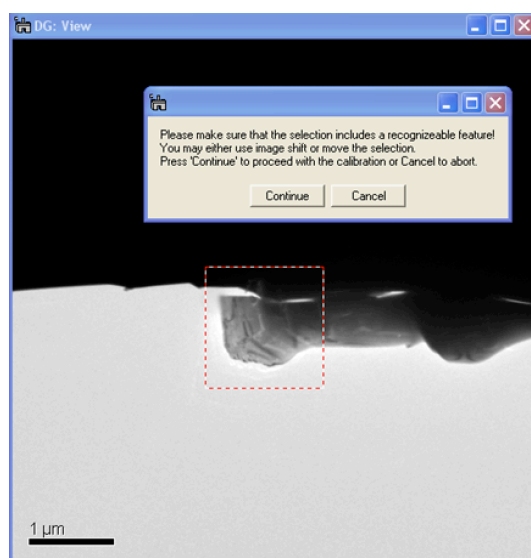


Figure 17: Screen shot showing an example of how a trackable feature may be selected in the View window that opens when the **Measure Imaging Aberrations** button is pressed.

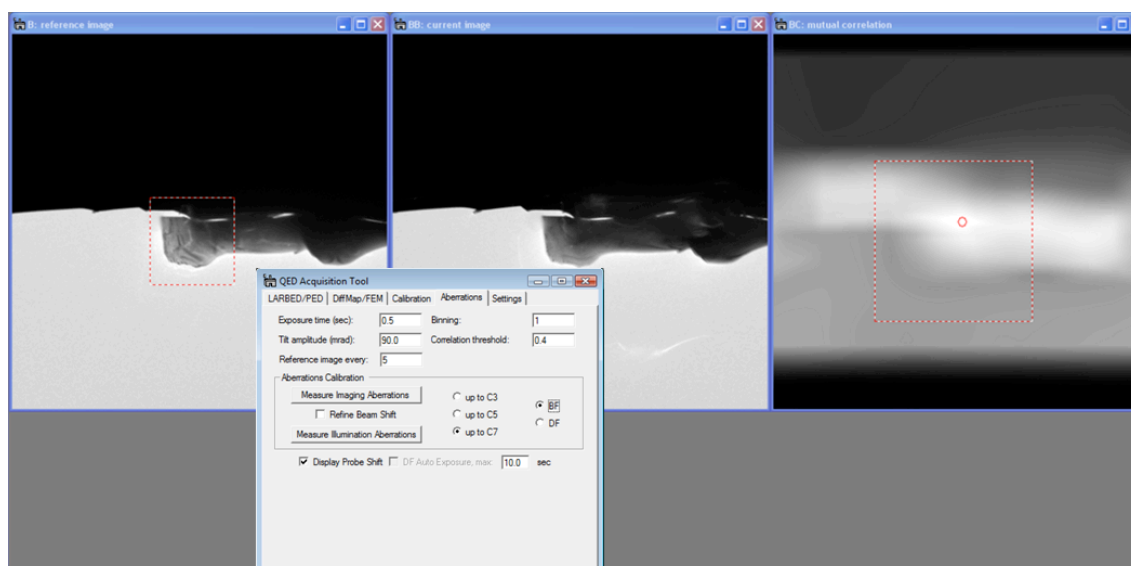


Figure 18: Screen shot of the image aberration calibration module in action. The relative shift between the current image and the reference image is kept small because of the compensation of the image shift according to the dynamically updated pseudo aberration coefficients.

Because the tilt-induced image shift can be quite large (several  $\mu\text{m}$ ), this automated calibration routine will predict the image shift at the next beam tilt and compensate it as much

as possible. It does so based on the current estimate of the pseudo-aberration coefficients that have been fitted to the measured image shifts of the images already acquired. As the number of acquired images increases so does the accuracy of these preliminary coefficients and with that the accuracy of the predicted image shift. The calibration routine therefore changes the beam tilt in a spiral pattern, starting with small beam tilts and gradually increasing its magnitude (see Figure 19 for the numerical values of the applied beam tilt). This procedure ensures that the area of the sample being tracked remains within the field of view of the detector even for very high values of the pseudo-aberration coefficients (see Figure 18). During calibration the current beam tilt, measured image shift and applied shift compensation will be displayed in the results window (see Figure 19).

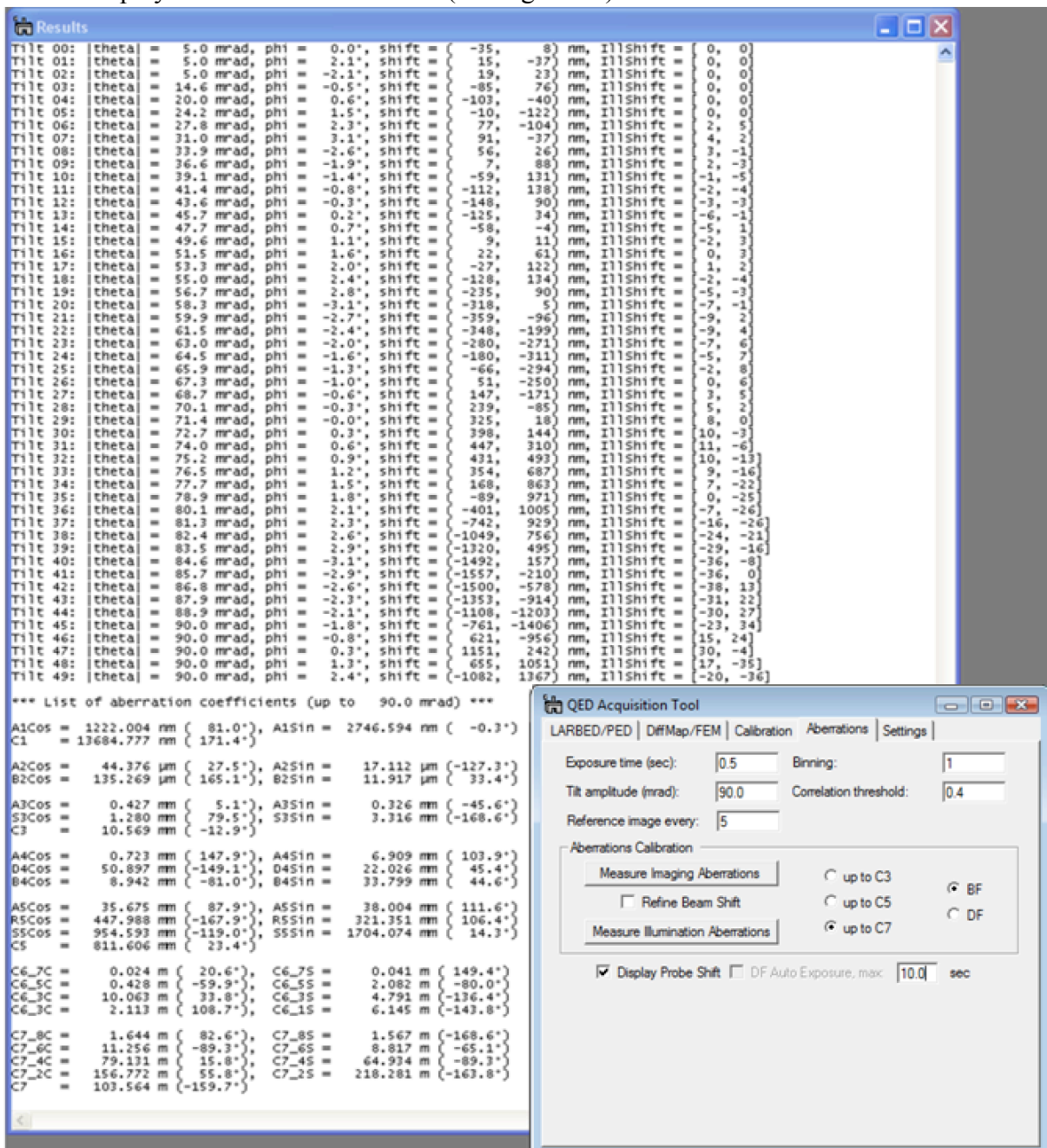


Figure 19: Screen shot of the Results window after the measurement of a set of pseudo-aberration coefficients of the illumination system up to  $C_7$ . As each image is acquired, the corresponding tilt angle, measured image shift and applied beam shift (in DAC units) is printed to the results window. Finally, the list of fitted aberration coefficients is also printed to the screen.

### 5.3.2 Calibrating aberrations of the illumination system in **BF-mode**

Once the pseudo-aberration coefficients of the imaging system have been obtained, the aberrations of the illumination system may be calibrated in the very same manner, except that the specimen should be moved out from the field of view and a small condenser aperture should be inserted. The remaining procedure is exactly the same as for calibrating the aberrations of the imaging system. For measuring the aberrations of the illumination system, it is also important to have calibrated the beam shift, in addition to the image shift. If the **Display Probe Shift** option has been turned on the progress of the illumination aberration calibration is displayed graphically as shown in Figure 13. Once this step is completed, QED will print a list of the final pseudo-aberration coefficients as shown in Figure 19 and, we are, in principle, ready to acquire high-quality LARBED or PED patterns.

### 5.3.3 Refining the aberration calibration in **BF-mode**

Depending on the tilt range being used and the degree of linearity of the electron optics of the microscope the steps described in sections 5.3.1 and 5.3.2 may be repeated, but with the ‘**Refine Beam Shift**’ checkbox selected as shown in Figure 21. This setting will use the already existing set of pseudo-aberration coefficients of the illumination system to predict the beam shift necessary to keep the probe from moving on the sample while measuring the tilt-induced image shift (you must press the **Measure Imaging Aberrations** button to perform this measurement again). Since shifting the beam may also affect the beam tilt, the image-shift response may be slightly different than when this calibration was done for the first time, i.e. without compensation of the illumination aberrations.

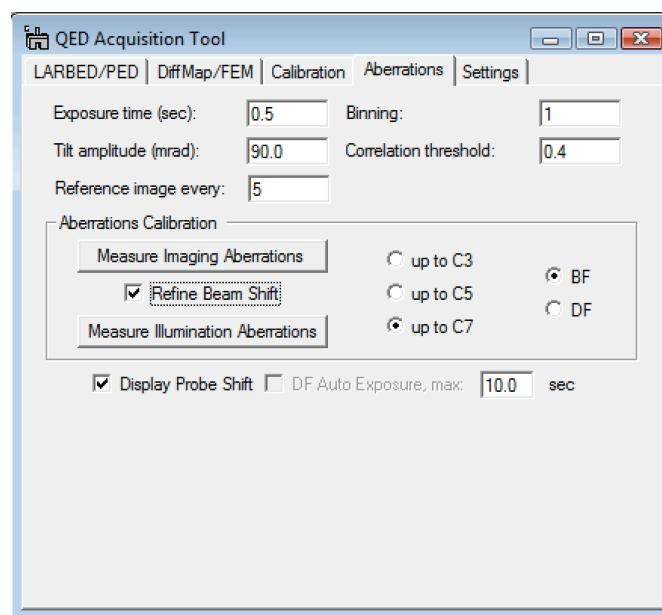


Figure 20: Screen shot of the **Aberrations** tab with ‘**Refine Beam Shift**’ turned on. This setting will apply the beam shift necessary to keep the illumination in the same position (as determined from the already existing set of pseudo-aberration coefficients) when measuring the tilt-induced image shift.

One may test the effect of the aberration compensation by acquiring a tilt series of images. Such a tilt series of images may be acquired from within the **DiffMap/FEM** tab (see Chapter 7). The example shown in Figure 21 demonstrates the great improvement in beam position caused by the dynamic aberration compensation. In fact, much of the change in Figure 21b



with tilt angle is due to the fact that these images are slightly different 2D projections of a 3-dimensional sample. If the result is still not satisfactory, the aberration calibration may also be refined further by repeating the procedure described in this section again. One should keep in mind though that, depending on the microscope, the precision with which the beam shift is being compensated may also be limited by the coarseness of the DAC that DigitalMicrograph may control. On Zeiss Libra TEMs, for example, remote control of the beam shift via the RS232 connection allows it to be changed in increments larger than about 20 nm., but on JEOL and FEI microscopes these increments are much smaller.

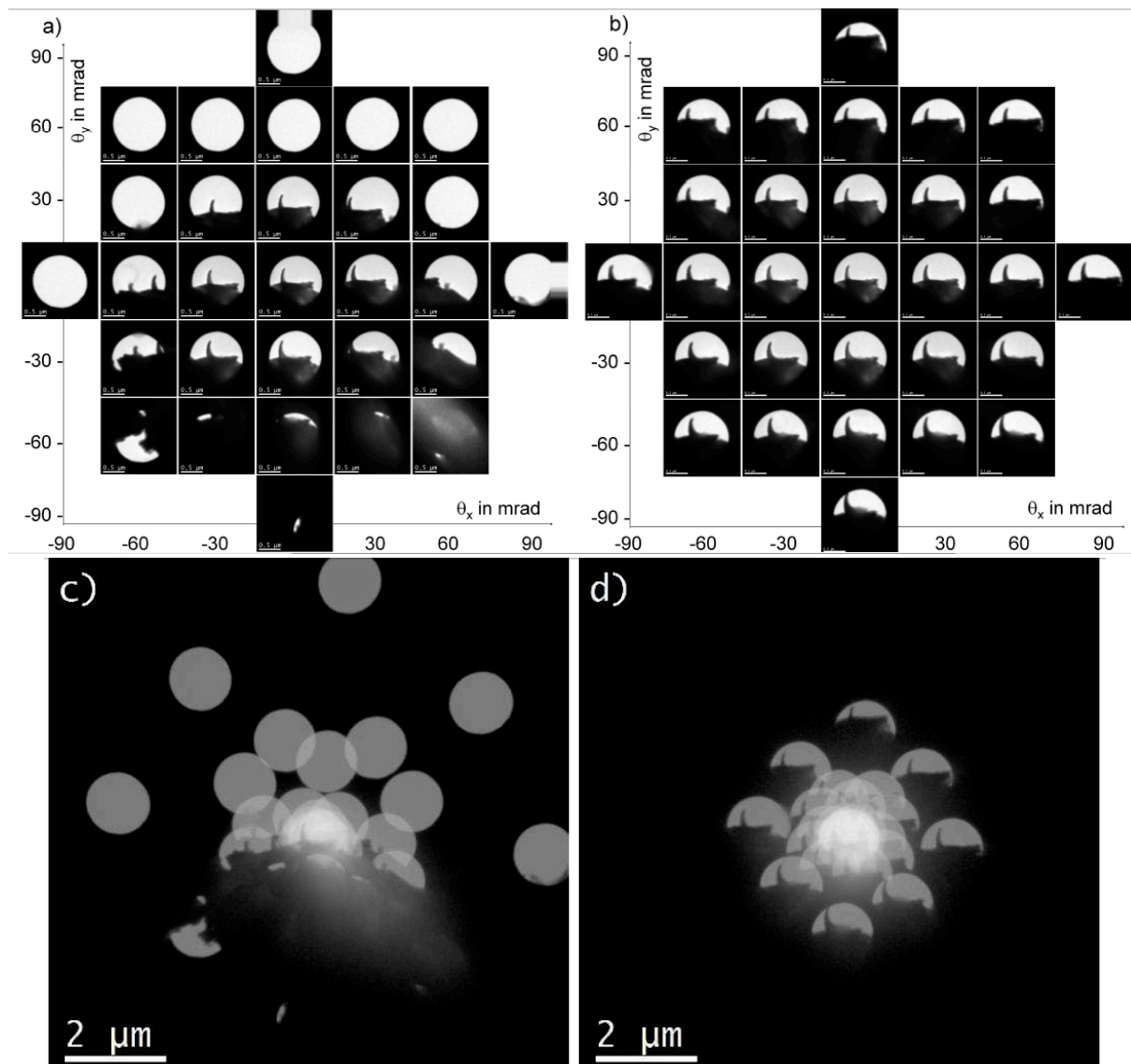


Figure 21: Demonstration of the effect of compensating the aberrations and tilt scan distortions of the illumination system. Images have been recorded for different illumination tilt angles, up to an amplitude of 90 mrad on a square 30 mrad grid. In the top row the areas that are illuminated by the electron beam at the different tilt angles are shown. Here only the portion of the image containing the illuminated area is shown. In the bottom row the sum of all 28 full-sized images is shown (on a log scale). a) and c) The aberration-induced beam shift has not been compensated for. b) and d) The aberration-induced beam shift has been compensated. Note that in d), because the imaging aberrations are not compensated the image still moves although the probe remains almost stationary on the sample. The origin of this effect is illustrated in Figure 15. The length of the scale bars in a) and b) is 500 nm. The accelerating voltage was 120 kV (Zeiss EM912).

#### 5.4 Measuring pseudo-aberration coefficients of the illumination system in **DF-mode**

As illustrated in Figure 14 the electrons (in the red beam) which travel down the optic axis of the microscope and intersect the objective back-focal plane at its center are not affected by any aberrations of the imaging system (by definition of the optic axis within isoplanatic approximation). Using only such electrons therefore allows the aberrations of the illumination system to be measured directly, no matter how strong the aberrations of the imaging system are.

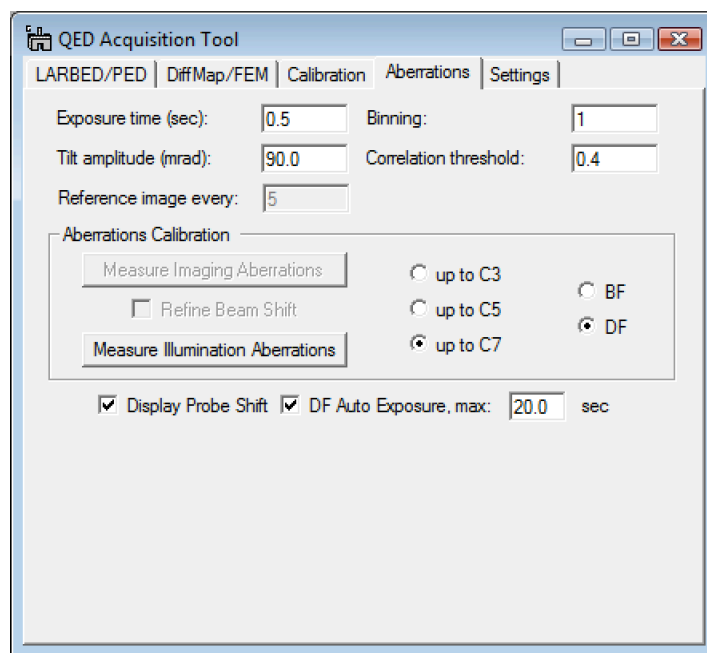


Figure 22: Screen shot of the **Aberrations** tab set up for a calibration of the pseudo-aberrations of the illumination system in **DF-mode**. Options which are only relevant to aberration calibration in BF-mode are made inactive.

As shown in Figure 22 a number of functions described in sections 5.3.1 – 5.3.3 are not needed anymore in **DF-mode**: It is not necessary to measure the aberrations of the imaging system, nor is it necessary to compensate any specimen drift. However, since we only want to detect electrons which have travelled along the optic axis of the microscope a **small objective aperture** is needed. Also, this calibration is best performed using an **amorphous specimen**, because amorphous structures are expected to scatter in all directions more or less homogeneously no matter how tilted the illumination may be. However, because the scattering of an amorphous sample along the optic axis may become very weak when tilting the beam to large angles, it may be necessary to adjust the exposure time for acquiring DF images. This adjustment is done automatically by QED if the **DF Auto Exposure** option is turned on. The **maximum exposure time** that may be used by QED however must then be specified as well (e.g. 20 seconds as shown in Figure 22). Note that, in order to perform the calibration as precisely as possible, QED will acquire two DF images at each beam tilt. It is important to keep this in mind when estimating the time this calibration procedure may possibly take.

The procedure for calibrating the illumination aberrations in DF mode is therefore as follows:

1. Setup the illumination conditions to the intensity and spot size desired for the actual LARBED or PED experiment.
2. Align the illumination tilt with the microscope's optic axis (rotation center)
3. Insert a small objective aperture and switch the microscope back to image mode
4. Adjust the exposure time and binning in the QED **Aberrations** tab to suit the intensity of the BF image, select the maximum exposure time for the auto exposure and press the **Measure Illumination Aberrations** button. It may be necessary to select a rather high binning, and a rather low magnification (10kx – 20 kx) in order to increase image counts at large beam tilts.
5. In the view window which then opens (similar to the screen shot shown in Figure 6, but for the spot recorded in Image mode), adjust the position (and size if necessary) of the ROI to contain the complete illuminated area and press **Continue**.
6. Watch the automated illumination calibration procedure. If you find that the algorithm cannot track the DF image of the illumination anymore (e.g. because the image counts are too few) you may stop the calibration procedure, adjust the experimental parameters (see hints given at step 4) and restart the calibration procedure. If the **Display Probe Shift** option has been selected a window showing the current estimate of the tilt-induced probe shift will appear after DF images for the first 5 tilt angles have been recorded.

## 6. Acquiring LARBED or PED patterns:

### 6.1. Acquiring integrated diffraction patterns

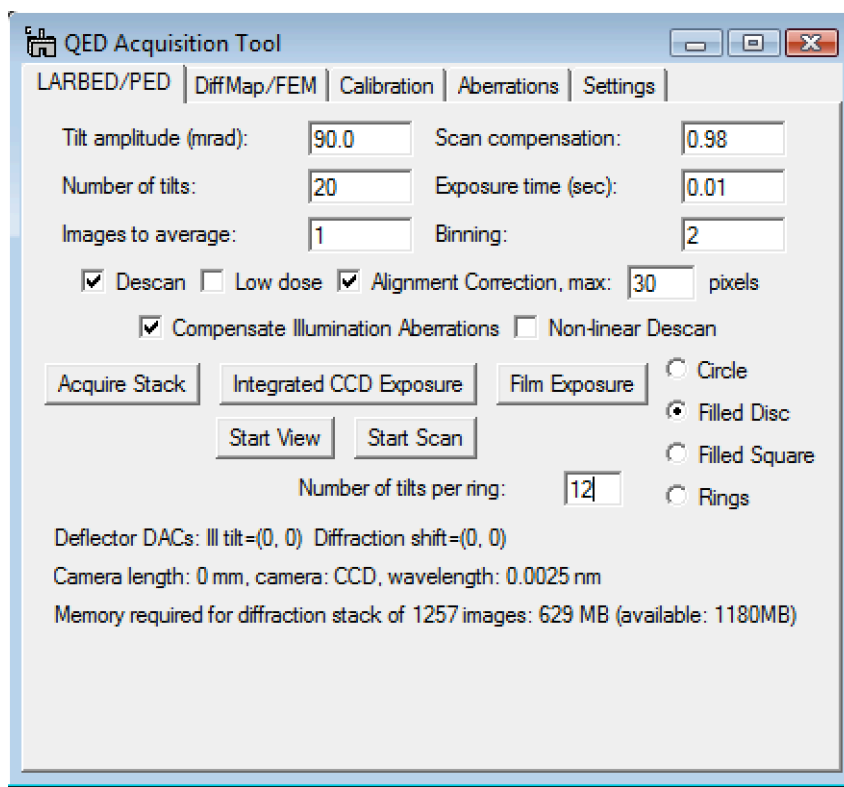


Figure 23: Screen shot of the **LARBED/PED** acquisition tab of the **QED Acquisition Tool**. It gives access to all the necessary experimental parameters affecting the Acquisition of LARBED and PED patterns.

Once the calibration is completed, the precession can be started and, if desired, viewed on the viewing screen by pressing **Start Scan** in the **LARBED/PED** tab (Figure 23). One may also acquire a single scan (ring, disc, or square) on the CCD detector by pressing **Integrated CCD Exposure**. Without a specimen in the path of the beam this may result in patterns as those shown in and .

*The acquisition of LARBED patterns may be interrupted at any time by pressing **Stop Scan** (the same button that was used to start the acquisition).*

The user may select between the 3 different shapes shown in Figure 24: a circle comprised of  $N$  points, where  $N$  is the value specified as **Number of tilts**, a disc comprised of approximately  $\pi N^2$  points (here the **Number of tilts** specifies the radius of the disc) or a square consisting of  $(2N+1)^2$  points. Unchecking the **Descan** box or setting **Scan compensation** to 0 will turn the de-scan off.

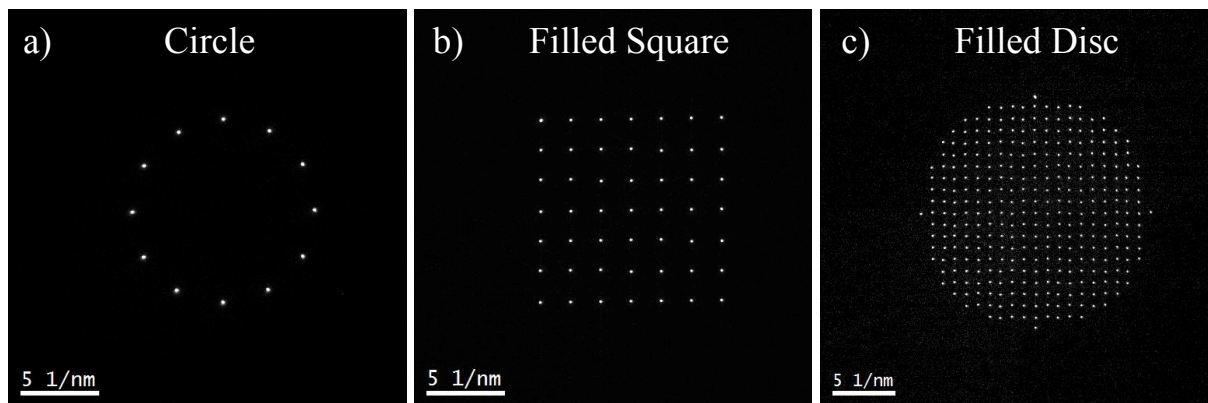


Figure 24: Example of the 3 different shapes for the illumination tilt scan recorded on the Zeiss SESAM 200 kV FEG-TEM: a) circle (here with 12 points and a camera length of 360 mm) b) square (here with the number of points set to 3, resulting in a total of  $(2*3+1)^2 = 49$  different beam tilts), and c) disc (here with a radius of 10 points). **Descan** and **Alignment Correction** were turned off in all 3 cases. The data has been acquired with the sample removed from the beam so that only the undiffracted beam was detected.

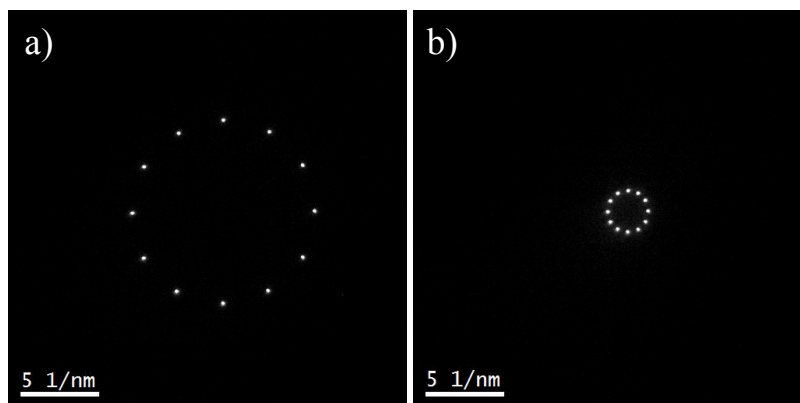


Figure 25: The same ring pattern of the undiffracted beam (sample was removed), recorded a) without any scan compensation and b) with a scan compensation of 0.8 (5 times reduced in size). The camera length was set to 360 mm in both cases.

shows the effect of changing the value of the **Scan compensation** from 0 to 0.8. You may note that the size reduction factor is given by  $1/(1 - \text{scan compensation factor})$ . Setting **Scan compensation** to 1 will result in a classical precession electron diffraction (PED) pattern. Figure 26 is a more practical example obtained with the scan compensation=0.84.

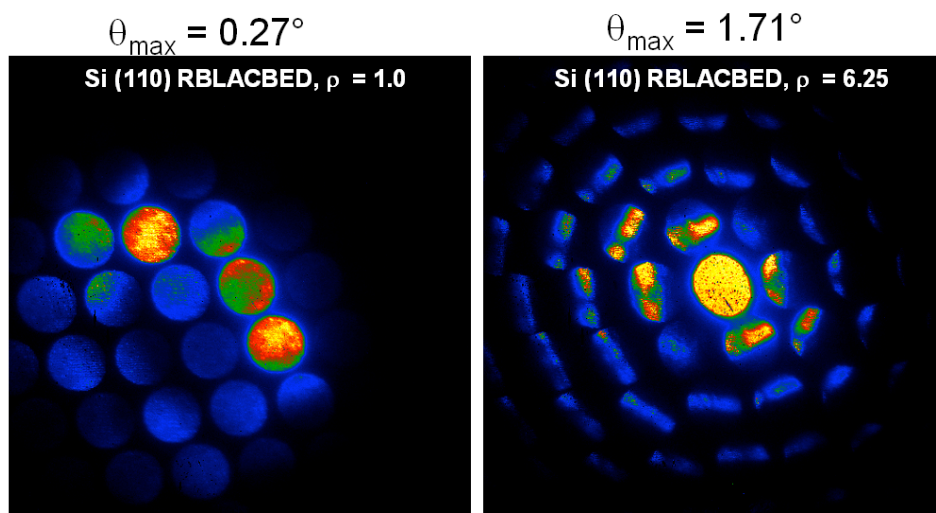


Figure 26: LARBED patterns of a very thin Si (110) sample produced by the software described here. The LARBED pattern shown on the left covers the same tilt range as a conventional CBED pattern (emulating a convergence angle =  $0.27^\circ$ ). Increasing the convergence angle in conventional CBED would cause the discs to overlap and disc-specific information would be impossible to extract. The right pattern shows diffraction data for the same position on the Si crystal, but with a 6.25 times larger effective convergence angle. The discs do not overlap here, because of the sequential acquisition and finely tuned de-scan provided by the QED plug-in (scan compensation=0.84, producing discs that are 6.25 times smaller than the tilt range they represent).

Figure 27 demonstrates the very different length scales within and between diffraction discs that results from the flexible choice of the **Scan compensation** parameter. Setting the scan compensation parameter to 0.9, for example, will make the scale within each diffraction disc 10 times smaller than the scale between the discs. As shown in Figure 27, a scan compensation parameter of 0.9 makes it possible to record diffractions discs with diameters of 20, 40 and 60 mrad. Without scan compensation each one of these discs would have greatly exceed the detector area.

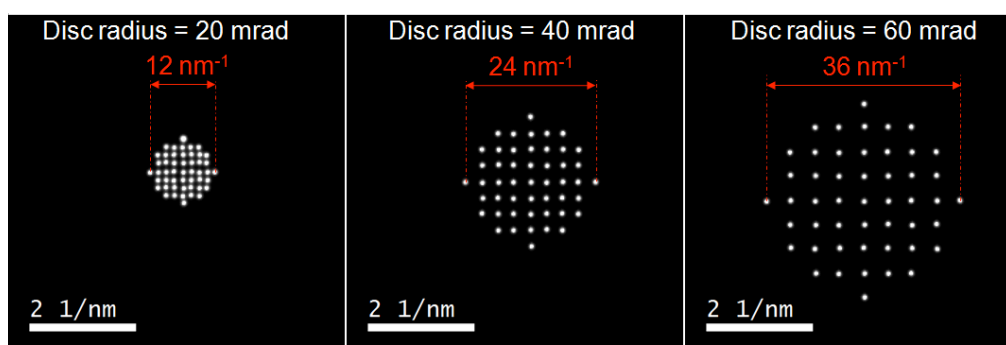


Figure 27: Disc scans acquired with the **Scan compensation** fixed at a value of 0.9 but different tilt amplitudes. Note the very different scales of the diffraction pattern (CCD calibration as indicated by the scale bar at the bottom left of each figure) and the disc diameter (as indicated above each disc). A scan compensation of 0.9 means that the discs have been reduced in size by a factor of 10.

## 6.2. Acquiring 3D data stacks:

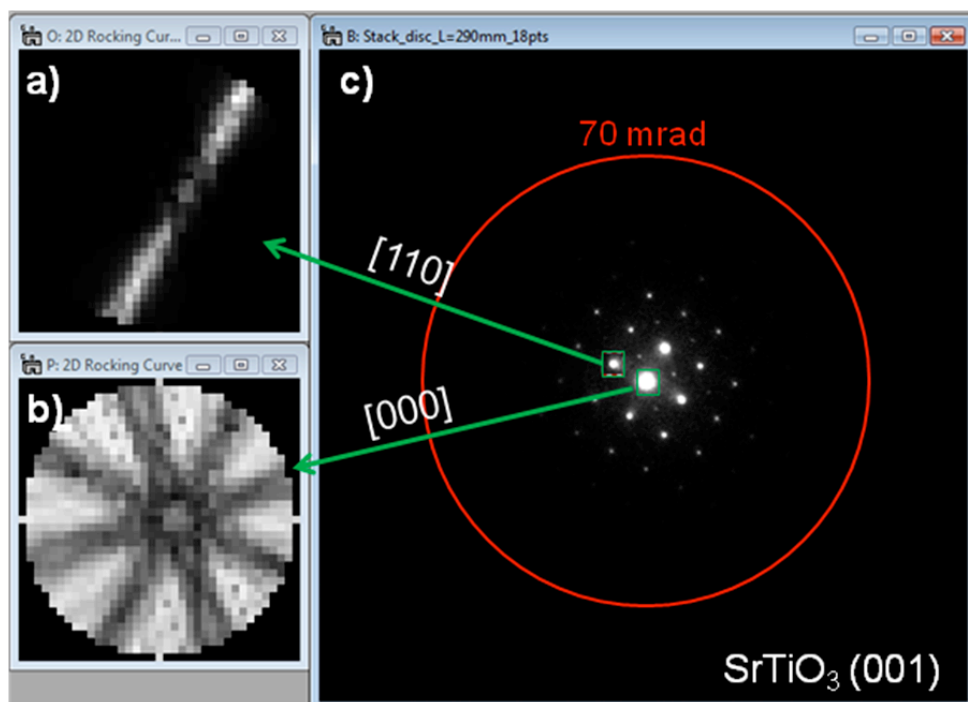


Figure 28: Example 3D data stack. a) and b) extracted diffraction discs. c) one of the frames of the 3D data stack comprising 1009 diffraction patterns (disc with 18 pixel radius). The red circle in c) indicates the range of tilt angles represented by the diffraction discs. The total acquisition time for this data stack was 23 min.

Much of the data reduction functionality provided in the QED menu are designed to extract diffraction information from 3-dimensional data stacks (see, for example, Figure 28). LARBED and PED 3D data stacks consist of individual diffraction patterns recorded at each incident beam tilt and may be acquired using the **Acquire Stack** button. This button works the same as the **Integrated CCD Exposure** button with the difference that in addition to the integrated diffraction pattern a data stack consisting of the individual patterns will be recorded.

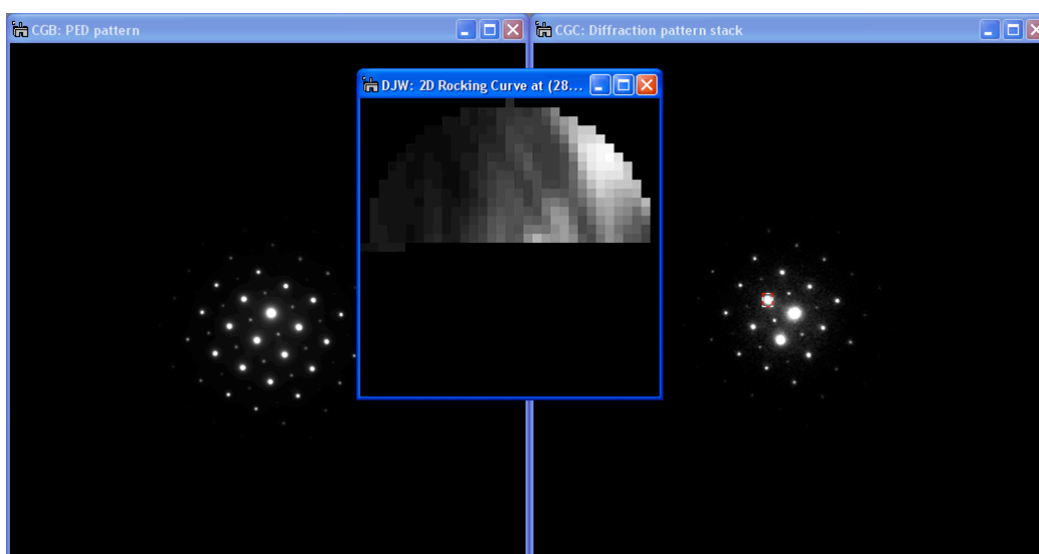


Figure 29: Watching the progress of the data acquisition by live extraction of rocking curves. During acquisition of a data stack two patterns are displayed: the integrated pattern on the left and the data stack showing the current frame on the right. Since the acquisition runs as a background thread, it is also possible to extract rocking curve information from the data stack during acquisition.

It is possible to start analyzing the data on-the-fly while the acquisition is progressing (see Figure 29). Although the progress is displayed numerically also at the bottom of the **LARBED/PED** tab, the **Display Rocking Curve** command from the QED menu will provide a graphical idea of how far the acquisition has progressed by showing a plot of the 1D or 2D rocking curve of a selected diffraction (Note: you must move or resize the selected area in order to update the rocking curve display.)

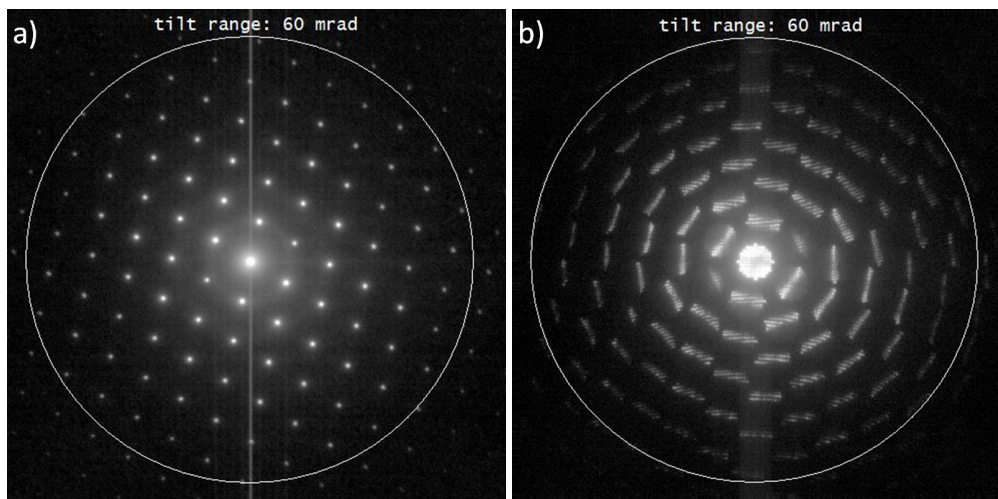


Figure 30: Comparison of two LARBED patterns of thin Si (110). a) pattern recorded with complete de-scan, b) pattern with only partial de-scan, both recorded on a Zeiss EM912 operating at 120 kV. The tilt range was 60 mrad in both cases (indicated by large circle). The aberration compensation was turned on for the acquisition of this data, so that all diffraction points stem from the same specimen position.

Figure 30 demonstrates another advantage of the acquisition of 3D data stacks. The data may then be projected in many different ways to produce either PED-like patterns (Figure 30a) or LARBED patterns (Figure 30b) which contain all the information from the 3D data stack in a 2D pattern.



### 6.3. Using the on-the-fly Alignment Correction:

During the simple tilt and descan calibration routine the software determines the direction and scale of the illumination tilt, and how much the diffraction patterns need to be shifted to compensate this tilt. Since this calibration assumes a linear behavior of the coils the actual pattern may look quite different, as can be seen in Figure 31, especially at large tilt angles.

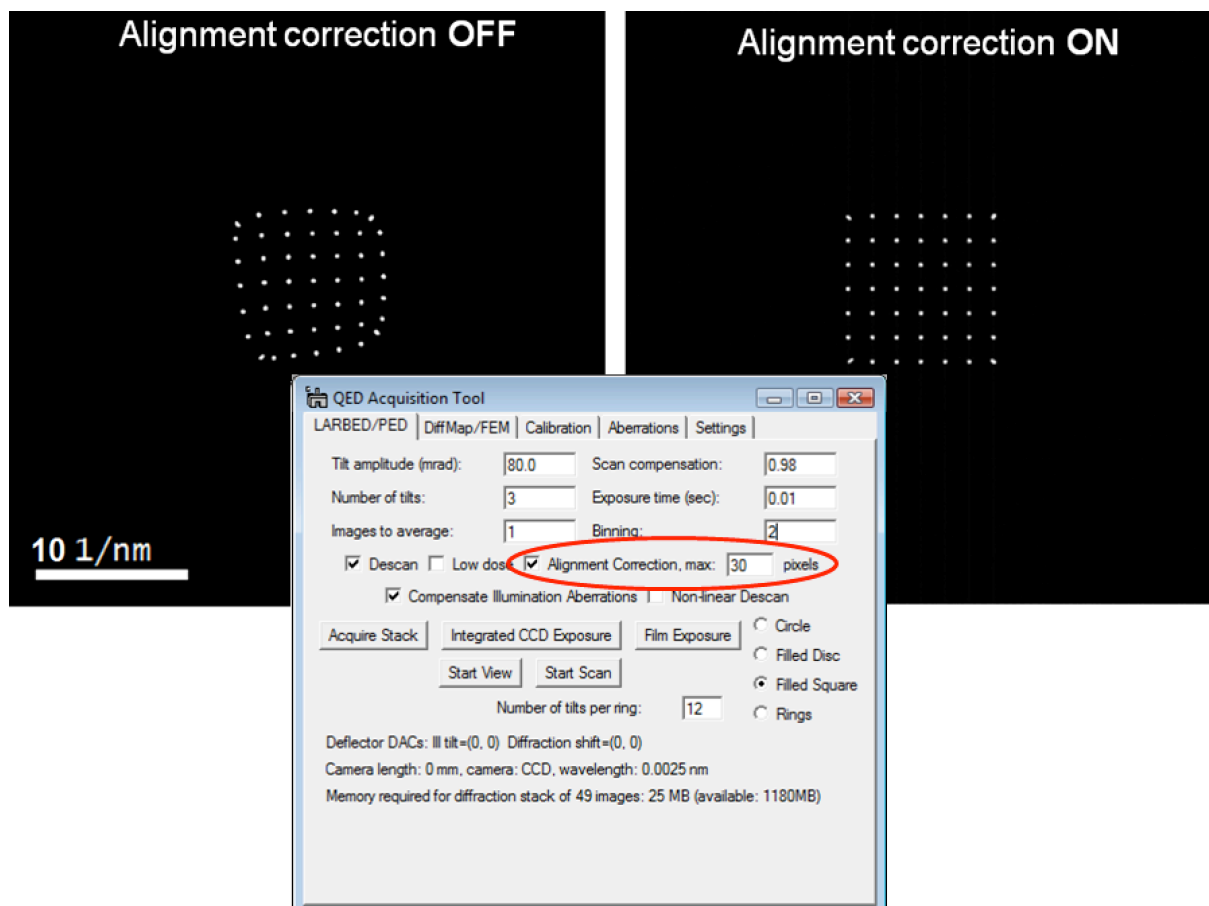


Figure 31: Effect of on-the-fly alignment correction: left: **Alignment Correction** was turned off, right: the **Alignment Correction** was turned on. Acquired on a Zeiss EM912 at 120 kV with a tilt range of  $\pm 80$  mrad in both x- and y-direction (note the distorted diffraction spots in the corners, where the beam tilt is 113 mrad).

As an alternative to applying the **Non-linear Descan** option, turning the **Alignment correction** “on” (highlighted in Figure 31) will make sure that the center of the diffraction pattern appears in the final LARBED or PED pattern or data stack at the proper position. This alignment is achieved by tracking the position of the central beam of the diffraction pattern. When the **Alignment correction** is turned “on”, the user is therefore asked to identify the central beam in an untilted diffraction pattern, which is acquired just before the actual LARBED or PED scan (see Figure 32).

The value next to **Alignment Correction** specifies the maximum number of pixels that the central beam drift is tracked for. If the beam drifts further than this, the correction will be aborted. One can, for example, estimate a proper value by testing this procedure without Alignment Correction and measuring the *uncompensated* maximum shift of diffraction patterns at high tilt amplitude (see Figure 33). Usually a value between 10 and 50 pixels should suffice (see also the **Align Stack** function below). Setting this value too high may

cause the central beam to be aligned with one of the diffracted beams (especially in thick samples).

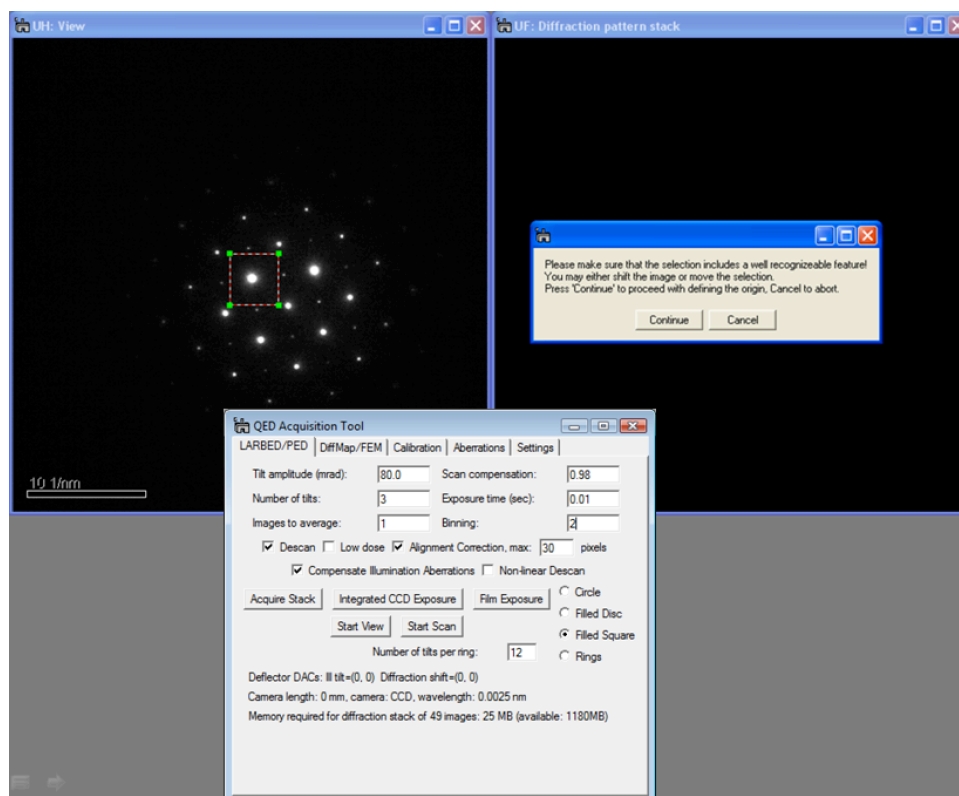


Figure 32: Screen shot demonstrating the procedure for identifying the central beam of the diffraction pattern. This procedure must be followed every time an acquisition is started for which **Alignment Correction** has been turned on. The alignment selection ROI will appear where it had been the last time. It may also be brought back to the center of the diffraction pattern by pressing the **Reset ROI** button in the **Calibration** tab. The diffraction pattern will be updated continuously, using the exposure time specified as **Exposure time**. It is therefore possible either to use the diffraction shift to bring the central beam into the selection ROI or to move (and re-size) the selection ROI to the position of the central beam.

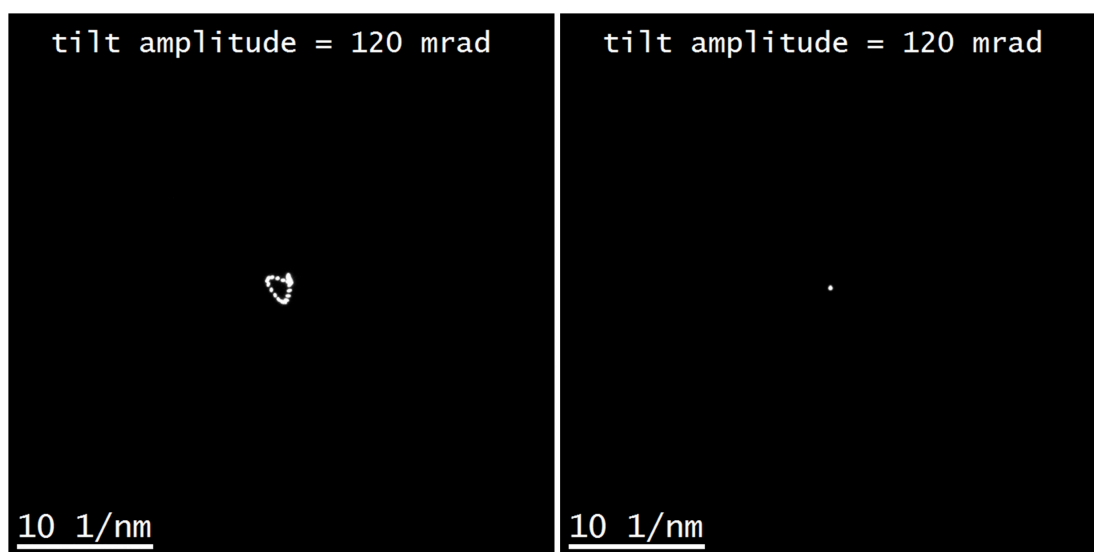


Figure 33: PED patterns recorded by the QED Plug-In on a Zeiss EM912 with a tilt amplitude of 120 mrad demonstrating the effect of the QED alignment correction. The left PED pattern has been recorded without alignment correction, and the one on the right with the **Alignment Correction** turned on.

## 7. Acquiring Drift Corrected Diffraction Maps and Fluctuation Microscopy data sets:

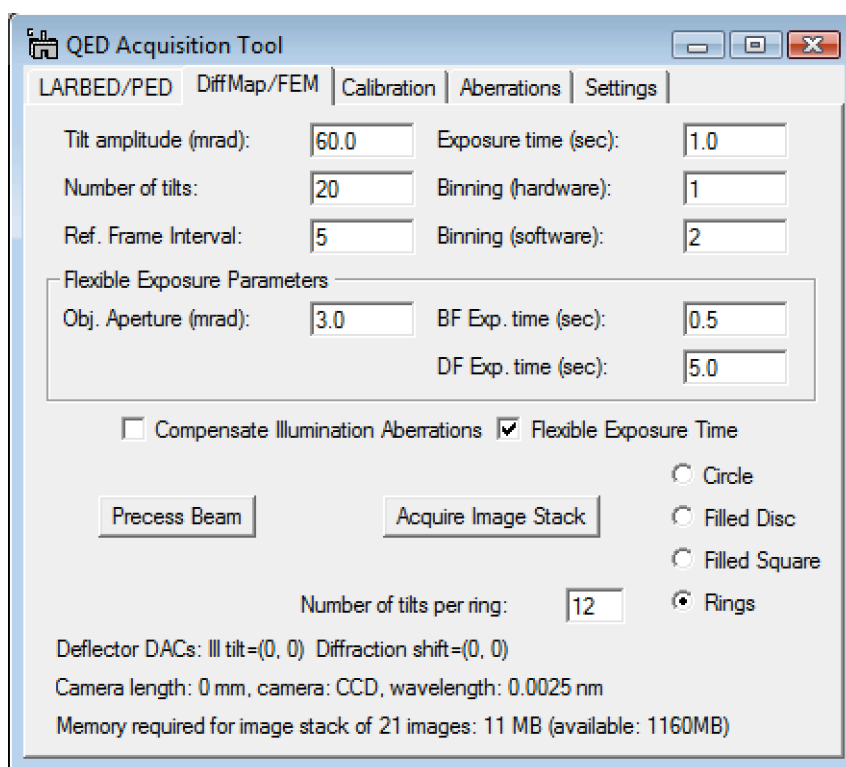


Figure 34: Screen shot of the **DiffMap/FEM** tab. In this example it is configured for a standard FEM acquisition, using the 'Rings' scan pattern.

Figure 34 shows the **DiffMap/FEM** tab of the QED Acquisition Tool. The control elements are very similar to those for the acquisition of diffraction data (LARBED/PED). The exposure time for images may generally be chosen much longer than for diffraction patterns, so these are two separate sets of parameters. Also, because dark-field images may have very few counts, the possibility of further binning of images by software is provided. While the maximum hardware binning is restricted by the CCD camera (some cameras allow a maximum binning of 4) there is no limit for software binning.

Because DF images can be quite low in intensity, acquisition times for such diffraction maps may be rather long, and the sample drift may be a limiting factor. However, by applying the on-the-fly drift correction provided by this DiffMap/FEM module, the sample can be kept within the field of view of the detector for many hours. The relevant parameter for drift correction is **Ref. Frame Interval**. It specifies after how many images it should acquire another reference image for compensating for specimen drift. Since DF images may change very much in contrast and certainly differ in contrast from BF images, reference images are always BF images recorded with the beam aligned along the optic axis. Once the drift between successive images has been determined and exceeds 10 pixels, the drift is compensated by sending the appropriate commands to the image shift coils. Image shifts of less than 10 pixels are compensated for by shifting the recorded image during the data reduction step.

The **Rings** scan pattern in the **DiffMap/FEM** tab (see Figure 34) was included with fluctuation electron microscopy (FEM) in mind. Recording a 3D data stack in this mode will result in a series of hollow-cone DF images with an equidistantly increasing precession angle. It is then just a matter of plotting the normalized variance of these images (or a selection thereof) to obtain the data necessary to perform a FEM analysis. (The routine for the FEM analysis will be added in a future release.) The number of tilts per ring is specified in the field next to **Number of tilts per ring**. The **Number of tilts** now specifies the number of different tilt angles, starting with  $\theta=0$  and finishing with  $\theta = \text{Tilt amplitude}$ . Note that for FEM applications a rather small **Number of tilts per ring** may be sufficient, since, at least ideally, amorphous structures scatter almost isotropically in all directions.

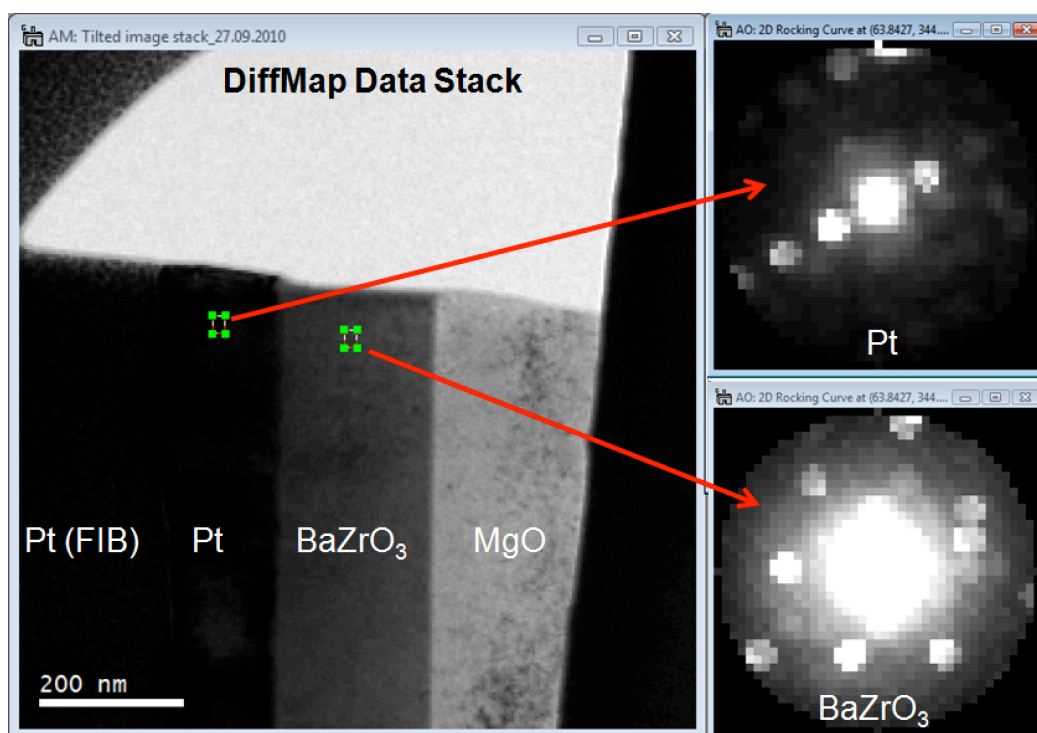


Figure 35: Example of a diffraction map of a multilayer sample. Moving or changing the size of the small ROI will automatically update the content of the locally extracted diffraction patterns.

Figure 35 provides an example of a diffraction map (DiffMap) recorded in real space. The automatic adjustment of the exposure time for BF images (beam tilt equal or smaller than radius of objective aperture) and DF images (beam tilt larger than objective aperture radius) allows all the images to be acquired in the same data stack. Note that also for the drift correction BF images with a potentially different exposure time than the DF images are acquired. Using the **Display Rocking Curve** function from the **QED** menu automatically compensates for differences in exposure time, so that diffraction patterns look as they would if acquired directly (without beam stop). The intensity of diffraction spots may therefore be measured on an absolute scale.

## **8. Some Basic Data Processing Functions:**

### **8.1. Post-acquisition alignment (**Align Stack**):**

Because of imperfect electron optics and a discretized control of the deflection coils, it is close to impossible to produce a perfect alignment of the diffraction patterns purely by commands sent to the microscope. This becomes quite obvious if looking at stacks of diffraction patterns recorded with full de-scan (i.e. '**Scan compensation**' set to 1). Moving through the slices of the data stack, one will notice the diffraction pattern moving slightly. This misalignment can easily be corrected by choosing the menu item '**Align Stack**'. The '**Align Stack**' function will first ask you to select an area that includes mostly the central beam of the diffraction pattern. This area should be chosen large enough to include the central beam in all slices of the stack. Once the "Continue" button is pressed the routine will align all diffraction patterns based on the content of this selection only.

It is important that the central beam is chosen, because all other diffracted beams may vary largely with incident beam tilt angle. This invariance of the intensity of the central beam with illumination tilt may also be used as a criterion to identify which of the beams is the undiffracted one. Turning 'Auto Survey' of the stacked image off in the Image Display Info Dialog (from Display -> Image Info...) and moving through the slices of the stack will show this very quickly.

In order to prevent the alignment routine to accidentally shift one of the diffracted beam to the position of the central beam, a (default) maximum allowed shift of 10 pixels is defined. This value may be changed by running the '**Align Stack**' function with the "Alt"-key pressed. Once this value has been changed, it will be used for all future alignments on that machine.

If the maximum shift has been set to too small a value, the diffraction patterns may not be completely aligned. The alignment can then be repeated once again (or several times).

Since the data alignment routine uses the position of the central beam as a reference, it also sets the origin of the diffraction pattern. It is then not necessary anymore to call the '**Define Origin**' function (see below) for the same diffraction pattern.

### **8.2. Undoing the stack alignment (**Undo Stack Alignment**):**

Working with large data stacks it is very important to waist as little memory as possible. The stack alignment is therefore performed on the original data set. However, since the amount of shift is stored in the tags of the data stack, the original image positions can always be recovered. This can be done by simply pressing the '**Undo Stack Alignment**' menu item. The '**Undo Stack Alignment**' command will also reset the shift stored in the image tags. Pressing this button more than once will therefore not have any effect on the data.

Note that this function will also remove the diffraction pattern shift applied during acquisition, if it has been recorded with the '**Alignment Correction**' option turned on.

### 8.3. Defining the center of the diffraction pattern (**Define Origin**):

The center of the diffraction pattern may also be defined without calling the alignment routine. The '**Define Origin**' command asks the user to select an area that only includes the central beam. It assumes that the data is relatively well aligned, and chooses the maximum of a smoothed average of all diffraction patterns (only the area selected by the user) as the center of the diffraction pattern.

### 8.4 Extract rocking curves of individual reflections (**Display Rocking Curve**):

The command **Display Rocking Curve** extracts 1D tilt scans or 2D rocking curves from data stacks. The rocking curves will automatically update with repositioning or resizing the region of interest.

In Figure 36 and Figure 37 you will find two examples of how this function works. Since all the acquisition parameters are stored within the tags of the image, the **Display Rocking Curve** command automatically decides whether to produce a line plot (circular precession scan) or a 2D rocking curve. As can be seen from Figure 36, the LARBED method allows simultaneous acquisition of LACBED patterns for all reflections, even for materials featuring large unit cells. Also, if used in nano-beam diffraction mode and with aberration compensation turned on, the illuminated area movement may be orders of magnitude smaller than in conventional LACBED.

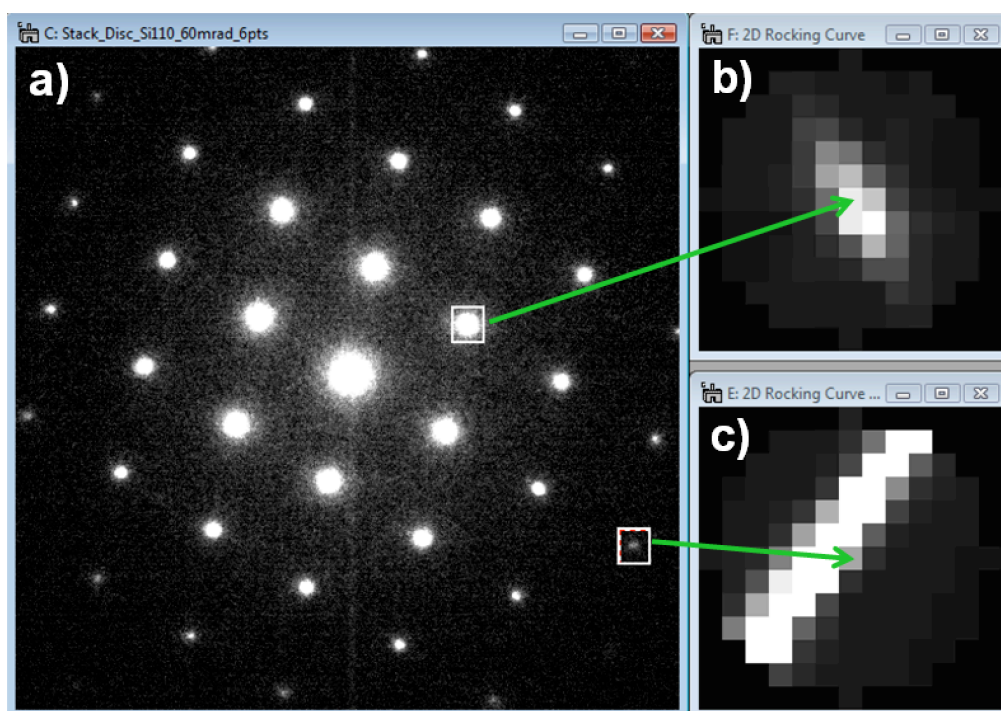


Figure 36: Extraction of LACBED discs from a LARBED data stack of Si (110) recorded using the 'Filled Disc' shape. a) Diffraction pattern corresponding to the central pixel of the extracted LACBED discs, as pointed to by the arrow heads in two extracted discs b) and c). The maximum tilt angle in these scans was set to 60 mrad. The accelerating voltage was 120 kV (Zeiss EM912). The intensity within the ROI (in this case, 23 x 26 pixels) was integrated in each diffraction pattern. The grey scale of the LACBED discs was set to b) -5000 ... 65900 counts (max. integrated intensity = 65998) and c) -1000 ... 14200 counts (max. integrated intensity = 26995). The data has been recorded with the aberration compensation turned on.

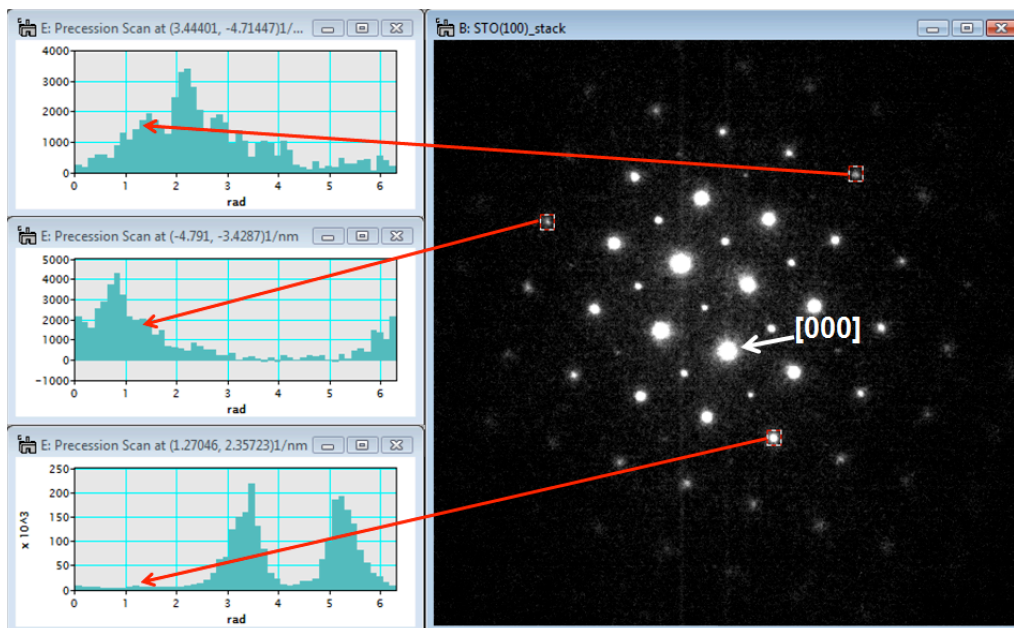


Figure 37: Example of the extraction of precession profiles from a LARBED stack acquired using a circular tilt scan from SrTiO<sub>3</sub> aligned near its (100) zone axis. The profile will be updated continually as the ROI is dragged around.

### 8.5 Produce table of diffraction intensities (**Print Rocking Curve**):

Calling the ‘**Print Rocking Curve**’ command will print a list of the integrated intensity within the selected ROI to the Results window in the form of a table.

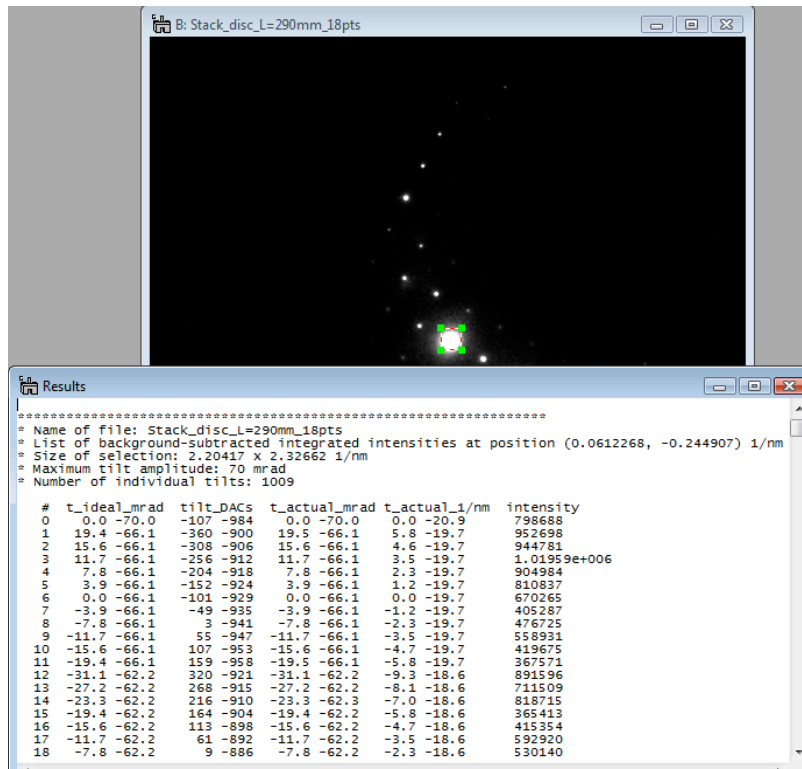


Figure 38: Example of a list of integrated intensities extracted from a LARBED stack printed to the Results window. The generated table can then be saved or copied to another number processing software. The different columns contain the intended (‘ideal’) beam tilt in mrad, the DAC units sent to the microscope and the actual tilt angle in both mrad and 1/nm. The final column contains the integrated intensity (background subtracted in the case of diffraction patterns).

### 8.6. Projections of PED/LARBED data (**Integrate Stack (?)**):

Having a set of all the diffraction patterns available, it is certainly easy to integrate over the different incident beam tilt angles by projecting the data stack along its depth, resulting in a single integrated diffraction pattern. This is simply done by pressing the ‘**Integrate Stack (?)**’ menu item. If the data stack has not previously been aligned, a warning will appear. However, this warning can also be ignored if that is what the user wants. Note that the small shifts induced by the alignment routine will also average over some of the noise introduced by correcting for the dark current. In some cases this may greatly improve the S/N properties of the PED patterns.

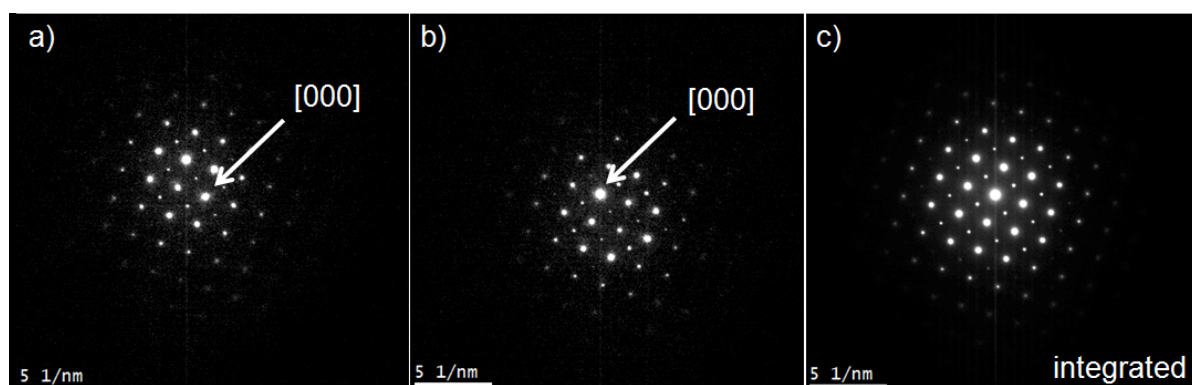


Figure 39 Diffraction patterns of SrTiO<sub>3</sub> (100): a) and b) two different patterns extracted from the LARBED stack. Note that the undiffracted beam is not always easily identifiable. c) Integrated diffraction pattern corresponding to a conventional PED pattern. This pattern is much more symmetric and also much less noisy than those shown in a) and b). Recorded on a Zeiss EM912, not energy-filtered.

### 8.7. Different projections of LARBED data (**Reconstruct LARBED Pattern**):

Integrating a data stack is only one of many possible projections. For this stack integration the patterns are summed up in the same position as they are present in the stack. Many more projections are possible, if the patterns are shifted before being summed. In this section we will show useful examples where this shift is proportional to the illumination tilt, with which each frame of a LARBED data stack has been recorded. Figure 40 shows an example of 6 different projections of the same LARBED stack, each projected by first shifting all the frames in proportion to the frame's beam tilt prior to integration.



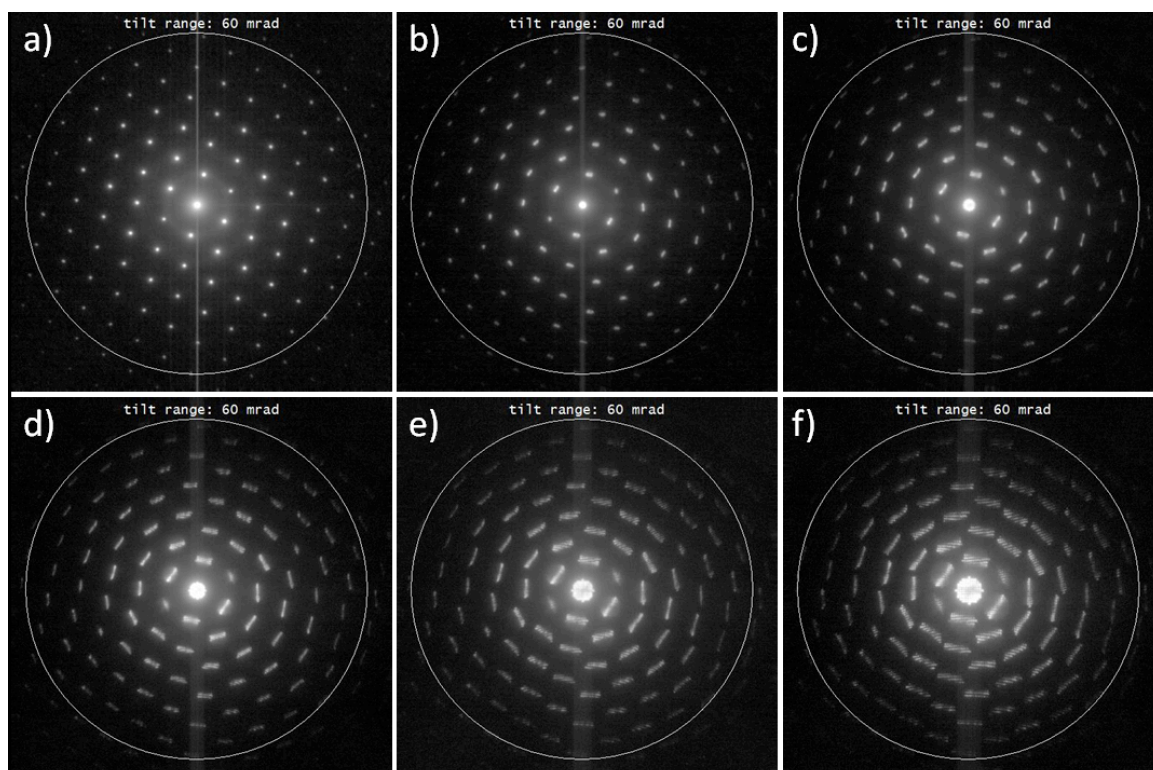


Figure 40: Different projections of a LARBED data stack recorded with full descans (**scan compensation = 1**) and a tilt range of 60 mrad (large circle superposed on each of the patterns). Pattern a) is equivalent to a simple stack integration and has been created by setting the scale of the diffraction disc to 0 pixels/mrad, and for pattern f) the diffraction disc scale was 0.2 pixels/mrad. Figures b) through e) correspond to equi-spaced intermediate diffraction disc scales between 0.04 and 0.16 pixels/mrad.

Figure 41 shows a screen shot of the **Reconstruct LARBED Pattern** command applied to a LARBED data stack (for producing the patterns shown in Figure 40). It is advised to align the data stack prior to executing this command (not always – see next example for extending the range of diffraction patterns for amorphous material). If the data has not been aligned the user will be prompted with a warning. The user may then select a scale for the circles, discs, or squares in pixels per mrad, depending on which scan pattern the data has been acquired with. Setting this value to 0 will produce the same pattern as the **Integrate Stack (?)** command. Leaving the default value will produce a pattern that appears as if no descans would have been applied at all. Setting this scale to, for example, 1/10 of the default value will produce a LARBED pattern in which the size of the scan pattern is down-scaled by a factor of 10, as is approximately the case in Figure 40f.

Once the scale of the diffraction pattern has been defined, the user is asked to define a threshold for the noise level, i.e. CCD counts below which data should not be included in the summation. If no such threshold shall be applied to the data, leaving the default value of 0 is fine.

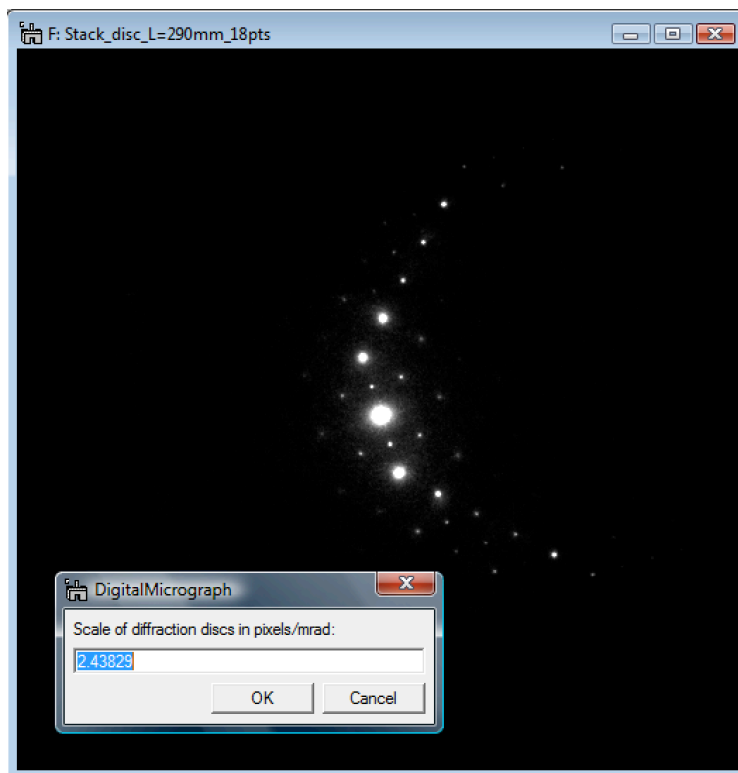


Figure 41: Screen shot of the **Reconstruct LARBED Pattern** command in action, results of which are shown in Figure 40. The initial value for the diffraction disc scale shown in the window corresponds to the scale, with which the data was acquired, i.e. applying this scale will make the diffraction discs as large as the white circles shown in Figure 40.

It is interesting to note that if the individual frames are shifted before being summed up, this shift enlarges the size of the reconstructed LARBED pattern. In some cases leaving the default value for the scale of the scan pattern (in pixels/mrad) may be very useful, as illustrated by the following example. Figure 42 shows how a large diffraction pattern may be assembled by a set of smaller ones, and, at the same time, the central beam has not been recorded (virtual beam stop). Here, the acceptance angle of the energy filter has been extended by compiling a larger diffraction pattern from a set of zero-loss filtered patterns covering a reciprocal space only about half as large.

For data like that shown in Figure 42 it is important to use the binary mask on each data frame in order to get a correct normalization factor. The similar mask that has been applied during acquisition may be used during reconstruction. Otherwise the averaging will be performed wrongly, resulting in a pattern like the one shown in Figure 42c. The position of the mask may be specified in two ways: a) by defining a threshold value, expecting that all intensity values within the aperture are above and those outside it below this threshold, or b) by defining (and selecting) a circular annotation in the data stack as shown in Figure 43.

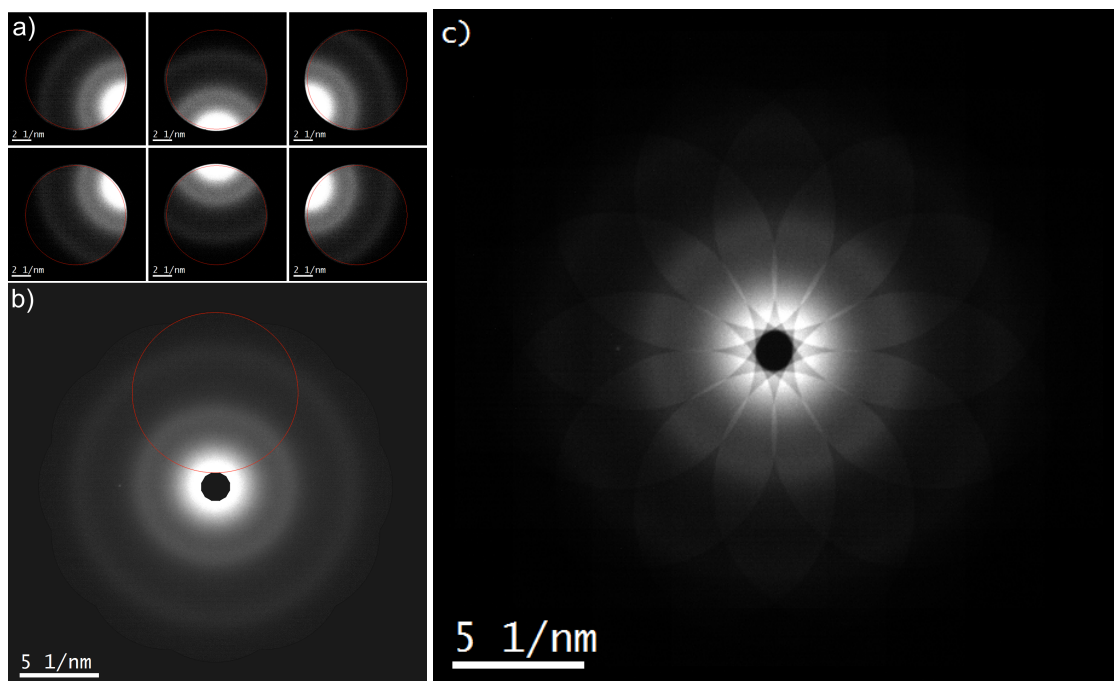


Figure 42: Reconstruction of a zero-loss filtered diffraction pattern of amorphous carbon from a LARBED data stack comprised of 12 partial patterns, each recorded with a large filter entrance aperture in place, blocking the central beam. a) 6 patterns out of 12. The circular annotation used to identify the area of interest has been superimposed on the data. b) Reconstructed pattern including normalization. c) Reconstructed pattern without applying normalization. Note that, depending on how much each of the diffraction patterns is shifted the reconstructed pattern has also more pixels than the original data.

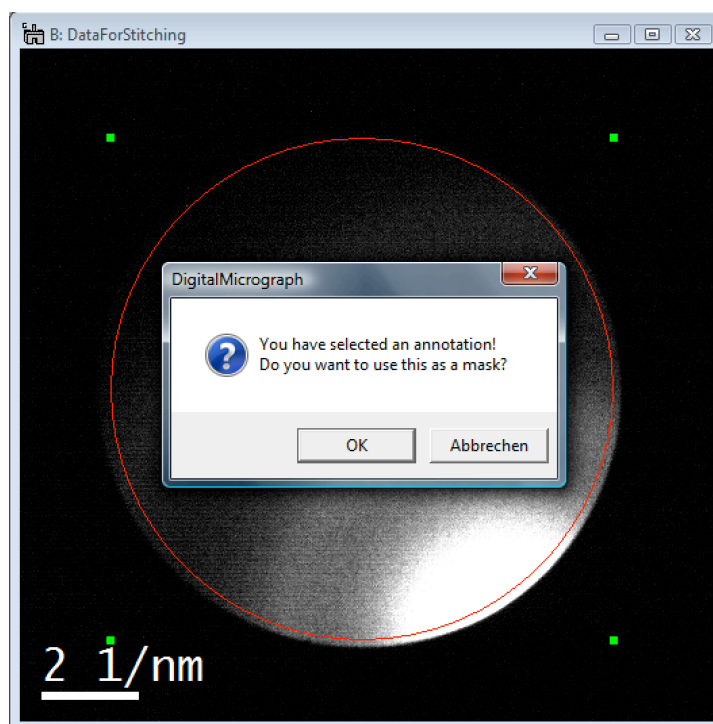
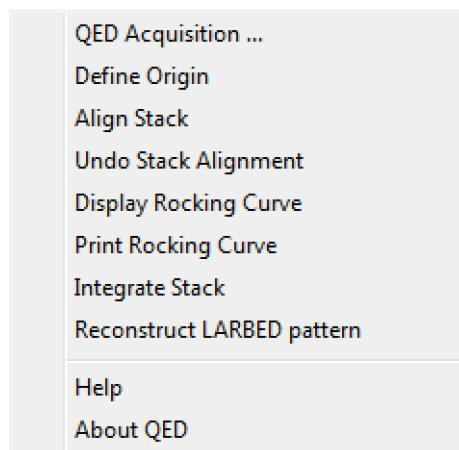


Figure 43: Screen shot of the **Reconstruct LARBED Pattern** command applied to a LARBED stack of amorphous carbon acquired with a large filter entrance aperture in place. The red circular annotation masks the range of valid data to be used for the reconstruction. Note that the annotation must be in the selected state in order to have any effect.

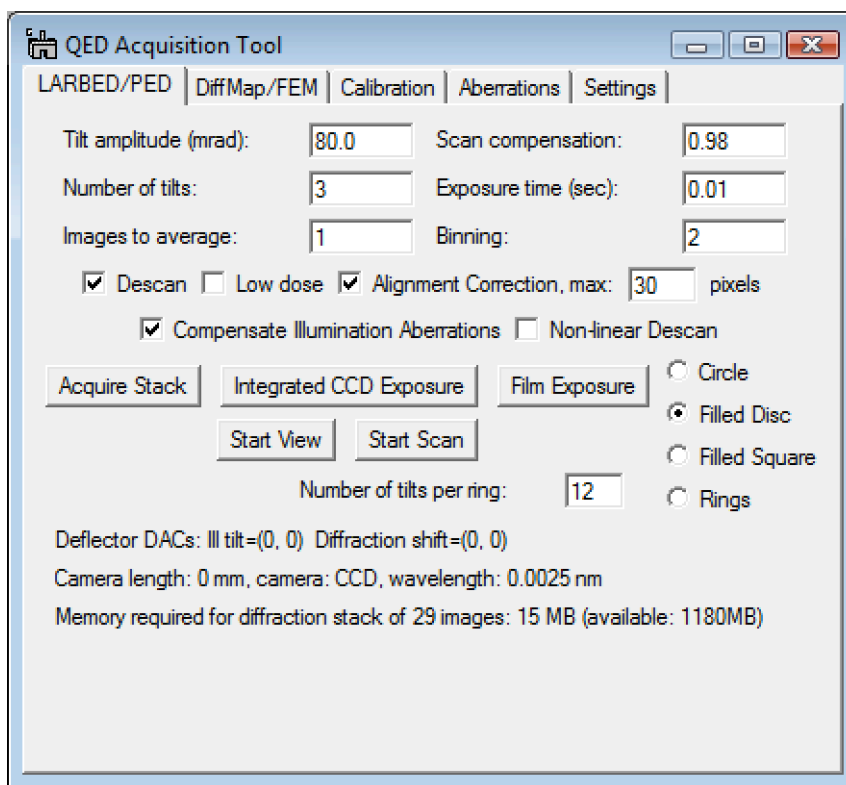
# QED Quick Reference Guide

## The QED Main Menu



Command	Description
QED Acquisition ...	This opens the QED Acquisition GUI (see below for details)
Define Origin	This defines the center of a diffraction pattern or diffraction data stack by locating the brightest pixel within an area selected by the user using a rectangular ROI.
Align Stack	This function automatically aligns stacks of diffraction patterns or images by tracking a well-recognizable feature. For LARBED or PED data stacks it is suggested to select the central beam using a rectangular ROI, since this will change the least with beam tilt (another feature must be selected if a beam stop has been used). Calling this function with the <i>Alt</i> -key held down will allow the user to specify a maximum shift.
Display Rocking Curve	<p>This function will display:</p> <ul style="list-style-type: none"> <li>- The 2D or 1D rocking curve of diffraction data stacks,</li> <li>- A local diffraction pattern of the selected region in the case of DiffMaps acquired with a disc- or square shaped scan pattern,</li> <li>- An azimuthally integrated 1D diffraction profile in the case of FEM (fluctuation electron microscopy - a ring scanned DiffMap), or</li> <li>- A plot of the fixed-tilt directional local diffraction intensity in case of a DiffMap with a circular scan pattern.</li> </ul> <p>The resulting plots or 2D patterns will be updated live, when the user-selected ROI is moved or re-sized.</p>

Print Rocking Curve	This function writes the information that would be displayed by the <i>Display Rocking Curve</i> function to the Results window.
Integrate Stack	This function integrates the 3D (PED/LARBED) data stack to create a 2D projection.
Reconstruct LARBED pattern	Computes a 2D projection of a LARBED data stack after shifting each of the recorded frames by a user specified amount. This function may be used to compile a larger diffraction pattern from a set of smaller diffraction patterns.

**The QED Acquisition GUI: The LARBED/PED Tab**

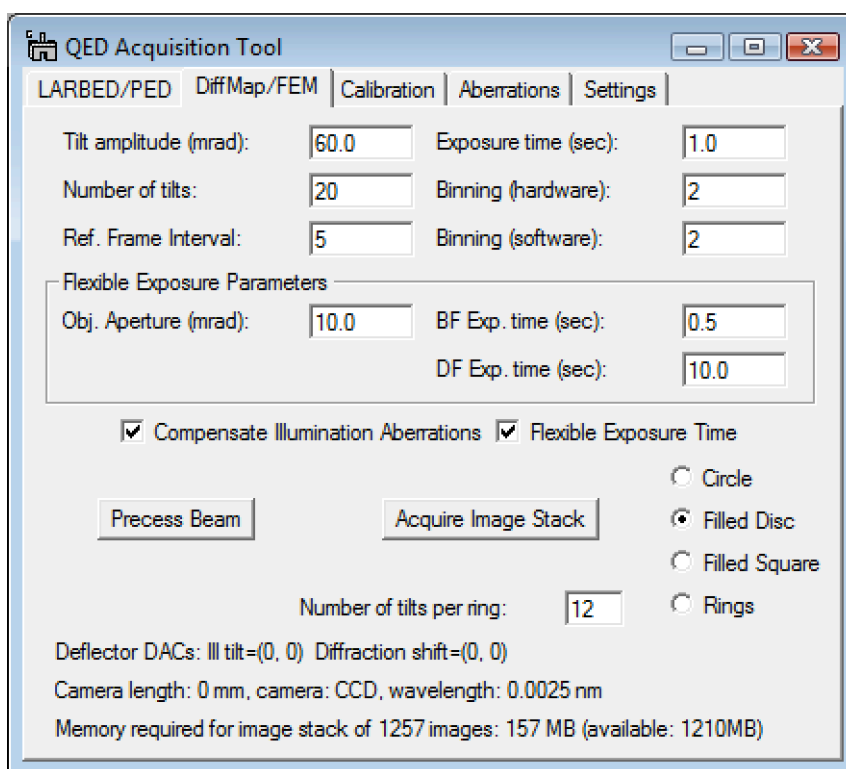
Command	Description
Tilt Amplitude (mrad)	The maximum beam-tilt angle corresponding to the radius of a circular scan pattern, half the width and height of the square scan pattern, or the radius of a precession circle.
Scan compensation	This specifies the relative portion of the beam tilt that will be compensated by the tilt de-scan. This value only applies when the de-scan is turned on. Setting this value to 1 will result in a classical PED pattern.
Number of tilts	Number of individual beam tilts around the circle in the case of circular scan patterns. For a disc-shaped scan pattern this specifies the number of tilts used to sample the disc radius. A square pattern will be sampled by $(2N+1)$ beam tilts where $N$ is the number of tilts. For a Rings pattern this specifies the number of concentric rings.
Exposure time (sec)	The exposure time used for individual CCD exposures or, in the case of exposing film, duration of individual beam tilt.
Images to average	Number of diffraction patterns that will be acquired and accumulated at each beam tilt.
Binning	Hardware binning applied when reading diffraction patterns from CCD.

Descan	This checkbox turns the de-scan on or off. If the de-scan is turned on it will be applied proportional to the beam tilt, scaled by the value given as the <i>Scan compensation</i> parameter.
Low dose	This checkbox applies mainly to the exposure of film (or image plates). If checked it will blank the beam between successive beam tilts, exposing the specimen for only the amount specified by <i>Exposure time</i> .  For acquisition on a CCD camera the user should select the pre-specimen blanker as a CCD shutter in order to minimize the dose on the sample.
Alignment correction	This turns on the de-scan correction for any imperfections and non-linearity in the (partial or complete) hardware de-scan by shifting the diffraction patterns to the proper position during the data acquisition. The maximum shift that will be compensated by this feature may also be specified. This value is the same as the one set in the <i>Settings</i> tab.
Compensate Illumination Aberrations	Ticking this checkbox will compensate for the tilt-induced beam shift, provided the illumination system has been calibrated.
Non-linear Descan	Specifies whether to use a simple linear de-scan calibration, or apply the calibration obtained when calibrating the shift-induced tilt.
Acquire Stack	Pressing this button will start the acquisition of a LARBED or PED data stack using the specified parameters.
Integrated CCD Exposure	Pressing this button will start the integration of the individual exposures at each beam tilt on CCD and obtain a LARBED or PED pattern in a single exposure.
Film Exposure	Pressing this button will acquire a PED or LARBED pattern on film. Because DM does not provide generic commands for film exposure this feature currently only works on Zeiss TEMs. Please contact us in case you are interested in acquiring such data on TEMs by other manufacturers.
Start View (Stop View)	This button starts a continuous CCD acquisition using the specified exposure time. The continuous acquisition will be stopped by pressing the same button (Stop View) again.
Start Scan (Stop Scan)	This button starts tilting and, if selected, compensating the beam tilt using all the parameters specified, just as for a regular exposure. However, no data will be acquired. The selected scan pattern will be repeated until the same button (Stop Scan) is pressed again.

Circle, Filled Disc, Filled Square, Rings	These radio buttons select between a simple circular precession (Circle), filled disc or square scan pattern (Filled Disc or Square), or a set of PED patterns with different precession angles (Rings). Note the difference in memory (shown at the bottom of this GUI) required for data stack acquisition in each of these modes.
Number of tilts per ring	This specifies the number of discrete beam tilt angles integrated over when acquiring the ring-shaped tilt pattern, e.g. for a sequence of PED patterns with varying precession angle. The number of concentric rings is specified by the <i>Number of tilts</i> parameter.



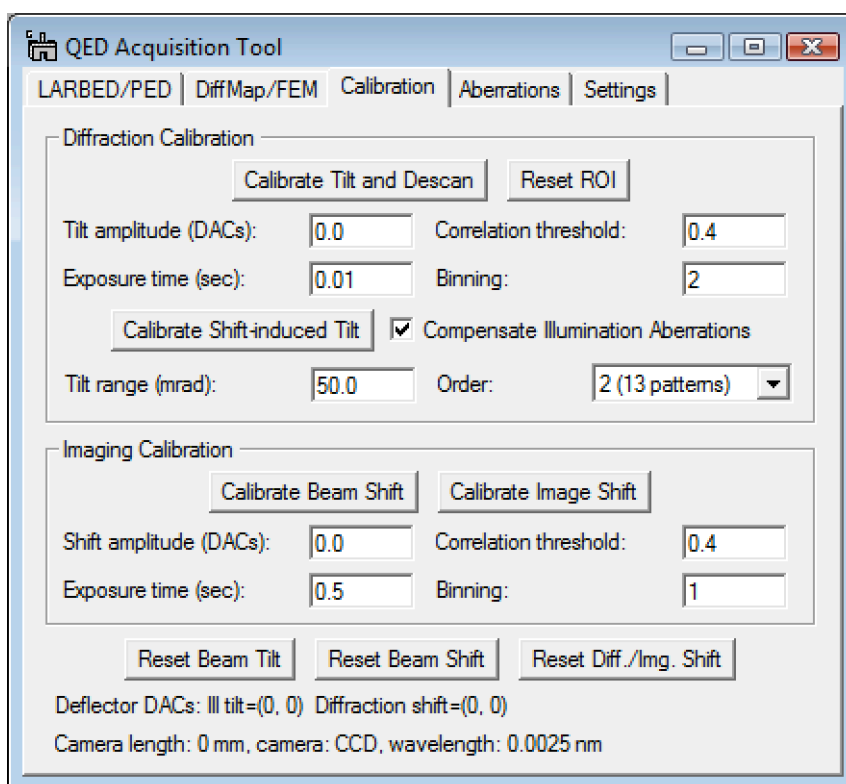
## The QED Acquisition GUI: The DiffMap/FEM Tab



Component	Description
Tilt amplitude (mrad)	The maximum beam-tilt angle corresponding to the radius of a circular scan pattern or half the width and height of the square scan pattern, or the radius of a precession circle.
Exposure time (sec)	This specifies a fixed exposure time for all images that will be used in case the <i>Flexible Exposure Time</i> feature is NOT selected.
Number of tilts	Number of individual beam tilts around the circle in the case of circular scan patterns. For a disc-shaped scan pattern this specifies the number of tilts used to sample the disc radius. A square pattern will be sampled by $(2N+1)$ beam tilts where $N$ is the number of tilts. For a Rings pattern this specifies the number of concentric rings.
Binning (hardware)	Hardware binning used to acquire individual BF or DF images.
Ref. frame interval	Number of data images acquired between successive BF reference images used for drift compensation. If this value is set to zero, then no drift compensation will be done.

Binning (software)	<p>In addition to hardware binning the acquired images may be binned further by software. Some CCD cameras support a maximum binning of 4. Software binning may then be used to reduce the data size of the final image stacks. Using a low hardware binning and high software binning also increases the dynamic range.</p> <p>Note that the image shift measurement and compensation is based on the as-acquired images, i.e. before applying software binning.</p>
Obj. Aperture	Specify the size of the objective aperture here if you want the <i>Flexible Exposure Time</i> feature to apply.
BF Exp. Time (sec)	The software will use this exposure times for BF images for which the beam tilt is within the objective aperture.
DF Exp. Time (sec)	The software will use this exposure times for DF images for which the beam tilt is outside the range of the objective aperture.
Compensate Illumination Aberrations	If you are using a field-of-view limiting condenser aperture, you may want to tick this checkbox in order to keep the illumination stationary with tilt. For a very broad beam this is not necessary. This requires, of course, that the illumination system have been properly calibrated beforehand.
Flexible Exposure Time	Tick this checkbox if you want separate exposure times for BF and DF images to be used.
Precess Beam (Stop)	This button starts precessing the electron beam but without acquiring images. This feature may, for example, be used to check whether the sample is properly focused. You can stop beam precessing by pressing the same button (Stop) again.
Acquire Image Stack	This button starts the acquisition of DiffMap or FEM data stack using the specified parameters.
Circle, Filled Disc, Filled Square, Rings	These radio buttons allow the selection of the desired scan pattern for the acquisition of diffraction maps (see section <i>Diffraction Mapping</i> for details).
Number of tilts per ring	This specifies the number of discrete beam tilt angles that will be integrated over when acquiring data stacks with the ring-shaped tilt pattern. This may find application in Fluctuation Electron Microscopy. The number of concentric tilt rings is specified by the <i>Number of tilts</i> parameter.

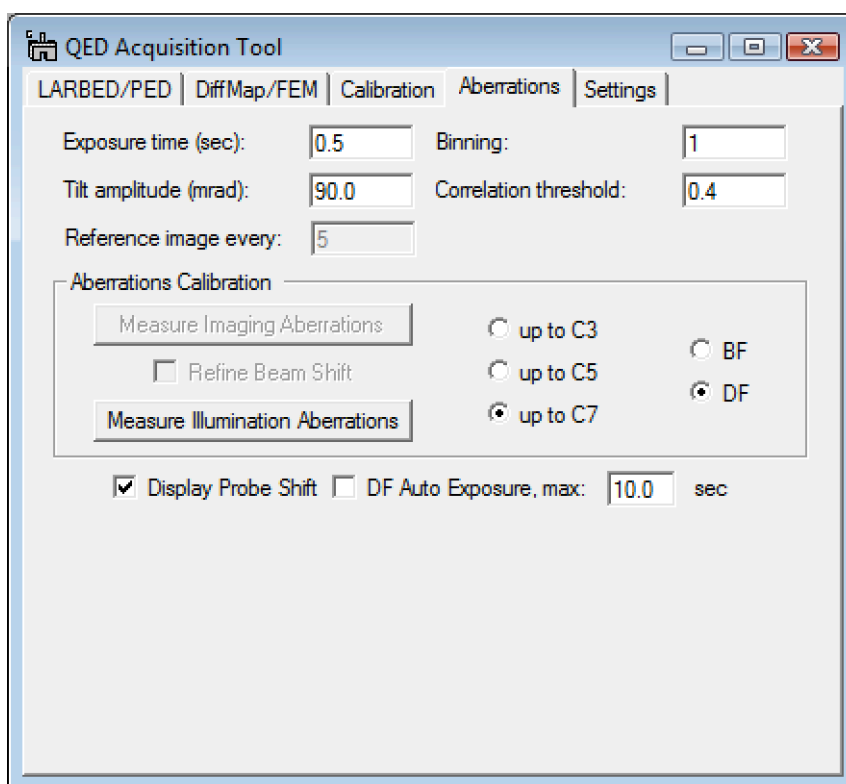
## The QED Acquisition GUI: The Calibration Tab



Component	Description
Calibrate Tilt and Descan	This button is one of the most important buttons of the whole GUI. It calibrates the beam tilt in mrad along X and Y and the diffraction shift necessary to compensate it.
Reset ROI	This resets the size of the region of interest (ROI) used to mark the area for tracking during the calibration routines to 1/8 of the size of the image and places the ROI to the center.
Tilt amplitude (DACs)	<i>It is recommended to leave this value at zero since in that case a suitable value will be estimated automatically.</i> In case you want a specific value to be used for beam-tilt calibration, you may enter the corresponding amount in DAC units here.
Correlation threshold (Diffraction/Imaging)	If the value of the correlation function used to measure relative image or diffraction pattern shift is below this value, the calibration routine will be aborted.
Exposure time (sec) (Diffraction/Imaging)	Exposure time used for acquiring diffraction patterns (in the <i>Diffraction Calibration</i> box) and images (in the <i>Imaging Calibration</i> box). Note that changing these values will also change the exposure times throughout this GUI.

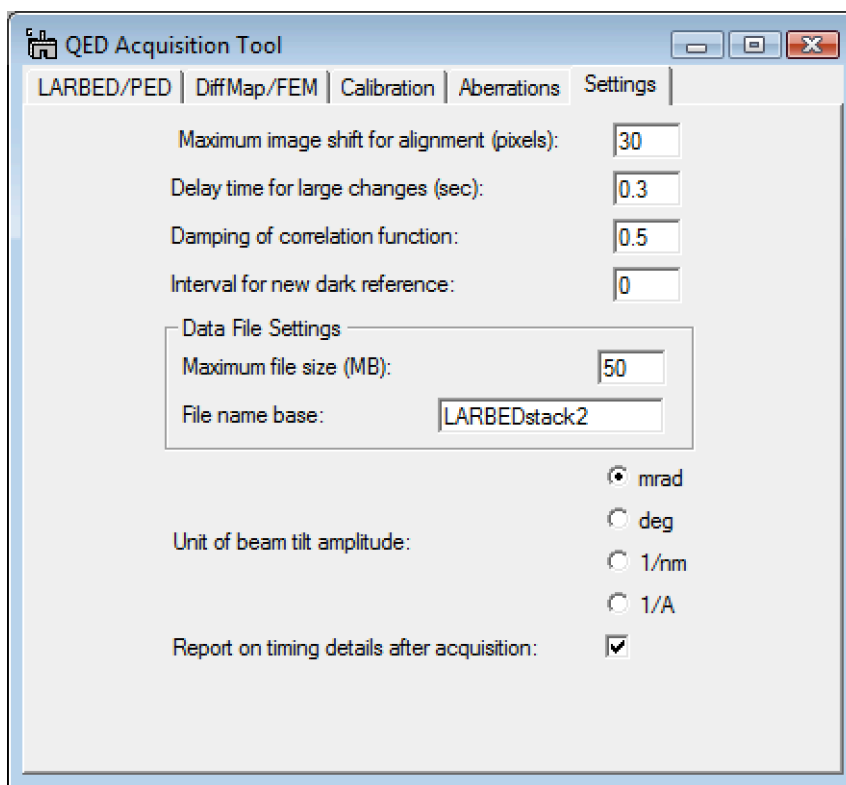
Binning (Diffraction/Imaging)	This defines the hardware binning used for acquiring the calibration data. These may again be different for images and diffraction patterns. Changing these values will also change the hardware binning throughout this GUI.
Calibrate Shift-induced Tilt	This button starts a detailed calibration of the de-scan coils which is much more reliable than the simple linear de-scan calibration (obtained by <i>Calibrate Tilt and Descan</i> ). If <i>Compensate Illumination Aberrations</i> is turned on, the tilt induced by shifting the beam on the sample is also compensated.
Compensate Illumination Aberrations	Selecting this option will apply the previously calibrated compensation of the illumination aberrations when calibrating the shift-induced tilt.
Tilt range (mrad)	This specifies the tilt range up to which the shift-induced tilt calibration shall be performed
Order	This selects the order of polynomial which will be fitted to the shift-induced tilt calibration.
Calibrate Beam Shift	This button starts the automated beam shift calibration routine necessary to perform the illumination aberration measurement. Start this with the sample removed from the beam and a small condenser aperture in place.
Calibrate Image Shift	This button starts the automated image shift calibration routine necessary to perform the imaging aberration measurement and drift correction during the acquisition of diffraction maps. Start this with an easily trackable feature on the sample at the center of the field of view.
Shift amplitude (DACs)	<i>It is recommended to leave this value at zero since in that case a suitable value will be estimated automatically.</i>  In case you want a specific value to be used for image-shift or beam-shift calibration, depending on which of the two buttons is pressed, you may enter the corresponding amount in DAC units here.
Reset Beam Tilt	This button resets the beam tilt to the value it had before the QED Acquisition GUI opened. This may be handy in situation when some unforeseeable event (e.g. communication problem between TEM and DM or a DM error message during acquisition) has halted the acquisition procedure and leave the beam tilt off-axis.
Reset Beam Shift	This button resets the beam shift.
Reset Diff./Img. Shift	This button resets the image shift or diffraction shift, depending on the mode of operation of the microscope.

## The QED Acquisition GUI: The Aberrations Tab



Component	Description
Exposure time (sec)	Exposure time used for acquiring all of the images used for fitting the pseudo aberration coefficients.
Binning	This defines the hardware binning used for acquiring the tilted images. Note that none of these images will be saved, so memory is not an issue here. However, a binning > 1 may increase the speed while sacrificing some accuracy.
Tilt amplitude (mrad)	Tilt amplitude up to which the tilt-induced image shift will be measured and the pseudo aberration coefficients will be fitted. Note that a default value will automatically appear when the order of aberration coefficient is changed.
Correlation threshold	If the value of the correlation function used to measure relative image shift between two images is below this value, the calibration routine will be aborted.
Reference image every	This specifies after how many tilted images the software should acquire a reference image (BF image) with the beam aligned along the optic axis. Recording a reference image frequently (e.g. every 5 frames) avoids the aberration calibration to be affected by specimen drift.

Measure Imaging Aberrations	This button starts the automated routine for measuring the pseudo aberration coefficients of the imaging system. It should be run without a condenser aperture and an easily trackable feature in the field of view of the detector.
Refine Beam Shift	This option should be selected when iteratively refining the calibration of the illumination pseudo-aberration coefficients. It will apply the previously determined beam shift when measuring the imaging aberrations in BF mode.
Measure Illumination Aberrations	This button starts the automated routine for measuring the pseudo aberration coefficients of the illumination system. It should be run with a small condenser aperture selected and no specimen in the field of view.
up to C3,C5, or C7	This specifies the degree of aberration polynomial being fitted to the tilt-induced image shift. This also affects the number of images that need to be acquired to allow fitting the corresponding number of aberration coefficients. Changing this selection will automatically suggest a corresponding default value for the tilt amplitude. Please see section on <i>Measuring Microscope Pseudo-Aberration Coefficients</i> for further details.
BF or DF	Selects whether the calibration of the illumination pseudo-aberrations should be performed in bright-field (BF) or dark-field (DF) mode.
Display Probe Shift	Produces a graphical display of the beam shift induced by the illumination pseudo-aberrations, as well as a graphical indication of the beam tilt angles already measured during illumination aberration calibration.
DF Auto Exposure	Selects whether QED may automatically adjust the exposure time in DF mode when the intensity of the DF images becomes too low. Maximum exposure time up to which the auto exposure mode may increase is specified in sec.

**The QED Acquisition GUI: The Settings Tab**

Component	Description
Maximum Image shift for alignment (pixels)	This value specifies the maximum shift between successive frames in a 3D data stack of diffraction patterns or images that will be compensated by the QED stack alignment routine as well as the on-the-fly alignment functions for LARBED/PED and DiffMap/FEM acquisitions
Delay time for large changes (sec)	This delay time may be necessary to allow for the deflector coils drivers to stabilize and depends on the microscope manufacturer. It will only be applied after the beam tilt and/or diffraction or image shift have been changed by large amounts (i.e. during calibration or before and after changing to BF condition for acquiring a reference image in DiffMap/FEM mode).
Damping of correlation function	This value specifies a damping function used to suppress high-frequency noise when aligning diffraction patterns and images. A value of 0.5 corresponds to Nyquist frequency and should generally be used.
Interval for new dark reference	For the measurement of the illumination aberrations in DF-mode this value specifies the number of dark-field images which will be acquired before a new <i>dark-reference</i> will be obtained. On some CCD cameras the scintillator after-glow requires new dark-reference images to be acquired every 5-10 frames if the signal of interest is very faint.

<p>Data File Settings</p> <p>Maximum file size (MB)</p> <p>File name base</p>	<p>If a data stack to be acquired exceeds the available memory (largest block of consecutive memory) or if a user wants to impose an upper limit on the size of data files produced by QED, it will be saved in blocks no larger than the <i>maximum file size</i> using file names which start with the name specified as <i>File name base</i>, appended by an integer index. The target directory will be specified by the user when starting the acquisition of a data set which requires saving in blocks.</p>
<p>Unit of beam tilt amplitude</p>	<p>Here the unit being used to specify the tilt amplitudes and angular cut-off of the objective aperture may be set up. Changing the unit will immediately change the values in all the affected GUI items.</p>
<p>Report on timing details after acquisition</p>	<p>Checking this box will print a detailed report on the time it took to move the beam and read the data from the CCD camera after each acquisition.</p>